CHARACTERIZATION OF THE NORSPERMIDINE-PREFERENTIAL ABC-TYPE TRANSPORTER POTABCD1 IN *V. CHOLERAE* BIOFILM FORMATION

A Thesis
by
ELIZABETH ANNE VILLA

Submitted to the Graduate School
at Appalachian State University
in partial fulfillment of the requirements for the degree of
MASTER OF SCIENCE

August 2016
Department of Biology

CHARACTERIZATION OF THE NORSPERMIDINE-PREFERENTIAL ABC-TYPE TRANSPORTER POTABCD1 IN *V. CHOLERAE* BIOFILM FORMATION

A Thesis
by
ELIZABETH ANNE VILLA
August 2016

APPROVED BY:

Dr. Ece Karatan
Chairperson, Thesis Committee

Dr. Ted Zerucha
Chairperson, Thesis Committee

Dr. Mary Kinkel
Member, Thesis Committee

Dr. Zack Murrell
Chairperson, Department of Biology

Max C. Poole, Ph.D.
Dean, Cratis D. Williams School of Graduate Studies

Abstract

CHARACTERIZATION OF THE NORSPERMIDINE-PREFERENTIAL ABC-TYPE TRANSPORTER POTABCD1 IN *V. CHOLERAE* BIOFILM FORMATION

Elizabeth Anne Villa
B.S. Virginia Polytechnic Institute and State University
M.S. Appalachian State University

Chairpersons: Dr. Ece Karatan, Dr. Ted Zerucha

The goal of this study was to further characterize the norspermidine and spermidine ABC-type transporter PotABCD1 in *V. cholerae*. Determination of the role of this transporter in biofilm formation is relevant to two very diverse phases of the *V. cholerae* life cycle: survival in the aquatic environment, and colonization within the human host. Biofilms have been shown to provide a colonization advantage in the mouse model, and may provide protection from harsh stomach and bile acid conditions encountered in the host prior to reaching the small intestine. This work identified PotA as an essential component of the norspermidine/spermidine ABC-type transporter PotABCD1 in *V. cholerae,* and determined that this transporter is strongly norspermidine-preferential. In this study I have shown that the *potABCD2D1* genes are arranged in an operon and that they are cotranscribed. I have also shown that mutations in PotA, PotB, PotC or PotD1 results in an increase in biofilm formation compared to wild type, indicating that spermidine uptake from the tryptone media has negative effects on wild-type biofilm formation. Finally, I have shown that biofilm forming ability may provide a colonization advantage in the zebrafish intestine, as biofilm-deficient mutants were

severely impaired in colonizing. This work further characterizes the novel norspermidine and spermidine transporter PotABCD1 in *V. cholerae* polyamine uptake, and provides insight into the role of this system in physiological aspects including biofilm formation and association with aquatic organisms.

Acknowledgments

I would like to acknowledge the Appalachian State University Office of Student Research, Graduate Student Association Senate, and Department of Biology for contribution of funds in support of this research. This research was also supported by the Grant A1096358-02A1 from the National Institute of Allergy and Infectious Diseases awarded to Dr. Ece Karatan. I would like to thank past and present members of the Karatan lab for their contributions to this work. I appreciate all suggestions and guidance provided by my committee members. I would like to extend a special thanks to my advisor, Dr. Ece Karatan. for her constant guidance, advice, and support. I have been so fortunate to have such an amazing mentor, and it has truly been a pleasure working with her.

Dedication

This work is dedicated to my amazing family, who have always supported and encouraged me in all of my pursuits. I would not be where I am today without you all.

Table of Contents

List of Tables

List of Figures

Introduction

Bacteria in the environment are thought to persist in sessile, multicellular and often multispecies communities known as biofilms (22). Cells in a biofilm are encased within a self-produced extracellular matrix (ECM) composed of polysaccharides, proteins, and extracellular DNA, and are physiologically distinct from the free-swimming form of the same organism (116). Bacterial biofilms may provide protection from a variety of environmental stressors, from UV irradiation and harsh pH to antimicrobials and immune responses (22, 27, 65). As such, biofilms may enhance both the environmental persistence of bacteria and virulence and survival within the host, especially for pathogenic microbes. Biofilm development occurs through specific and regulated steps, as shown in Figure 1. Cells first make contact with a surface or group of other cells and may form a transient attachment, but EPS production is required for mature biofilm structure development. Mature biofilms often exhibit a three-dimensional structure made up of pillars of cells and ECM interspersed with fluid-filled channels (21, 114, 116).

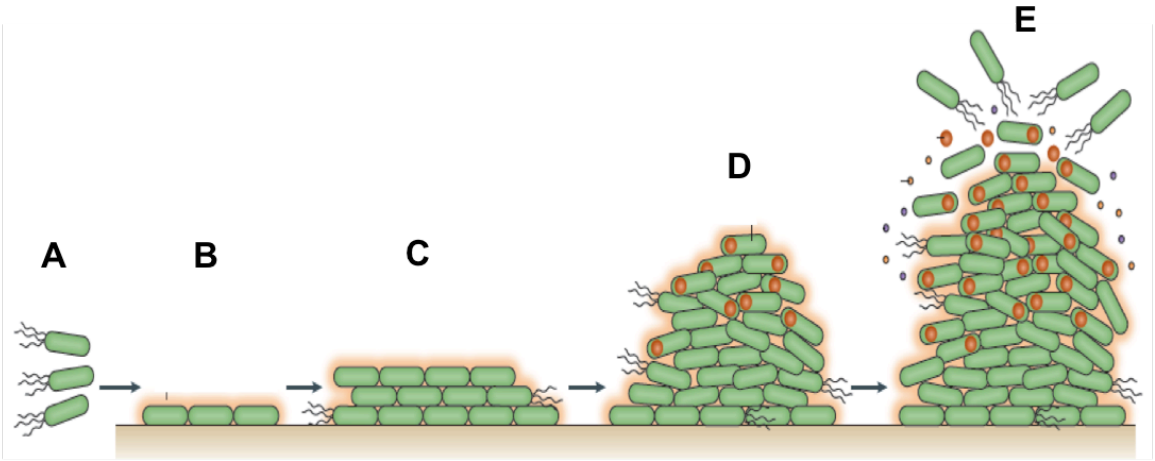

Figure 1. Development of bacterial biofilms. (A) Planktonic cells. (B) Surface adhesion and ECM production. (C) Growth and aggregation, 3-D structure formation. (D) Biofilm maturation. (E) Biofilm dispersal. Modified from Vlamakis *et al.* 2013.

A variety of signals and conditions may regulate the transition from the free-swimming state into the bacterial biofilm. Polyamines, small hydrocarbon chains with multiple amine groups, are one such group of signals (106). Polyamines are present in virtually all living cells. They have been indicated as regulators of a variety of physiological processes, and are essential for normal cell growth and function (106). The most commonly found cellular polyamines are putrescine, spermidine, spermine, and cadaverine. The structures of these polyamines, as well as norspermidine, a less common polyamine, are shown in Figure 2.

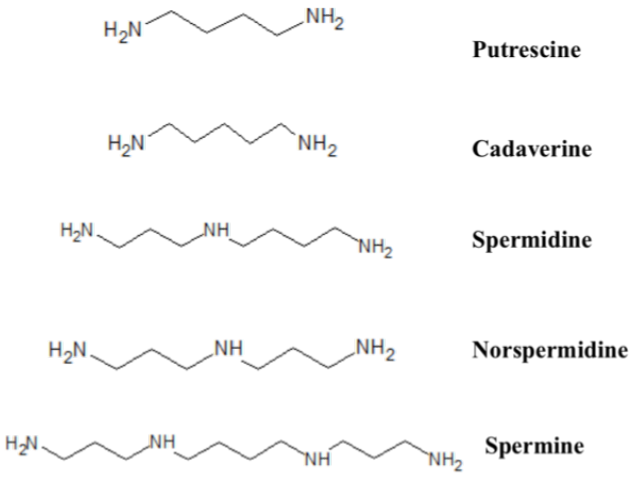

Figure 2. Structures of common intracellular polyamines in prokaryotes. Structures were drawn using ChemSketch and modified from Sanders, BE 2015.

Polyamines can regulate biofilm formation and many other physiological attributes through both extracellular and intracellular mechanisms. Polyamines outside of the cell may be recognized and responded to by regulatory systems, resulting in modulation of a second messenger, which then directly affects biofilm formation (51). One such molecule is cyclic-di-guanylate monophosphate (c-di-GMP). Levels of c-di-GMP are directly related to biofilm formation: increased c-di-GMP stimulates biofilm formation, while decreased levels of c-di-GMP reduces biofilm formation (9, 87, 112). Because they are positively charged at

physiological pH, intracellular polyamines are capable of binding to nucleic acids in order to modulate physiological effects. As such, intracellular polyamines are often found in a complex with RNA and may act as translational regulators (44). Spermidine in particular has been shown to bind to ribosomes and increase translational accuracy in wheat germ extract (47). Binding of spermidine to regions of mRNA may also result in structural changes in Shine-Dalgarno sequences, facilitating the formation of a transcription initiation complex in *E. coli* (127). A prokaryotic "polyamine modulon" has been proposed, encompassing genes that are transcriptionally regulated by polyamines. This mechanism suggests that polyamines do not simply regulate genes in an "on/off" manner, but rather modulate the level of expression of these genes in order to maintain ideal intracellular conditions for cell growth (45). However, excessively high levels of polyamines can become toxic to cells; for example, intracellular accumulation of spermidine has been shown to inhibit protein synthesis, which may reduce cell viability (29). Therefore, polyamine concentrations within cells are maintained at an optimal level through processes including import, biosynthesis, degradation, and excretion. Common polyamine biosynthesis pathways are shown in Figure 3, although these are not ubiquitous, and significant variation exists in polyamine biosynthetic pathways between and among species.

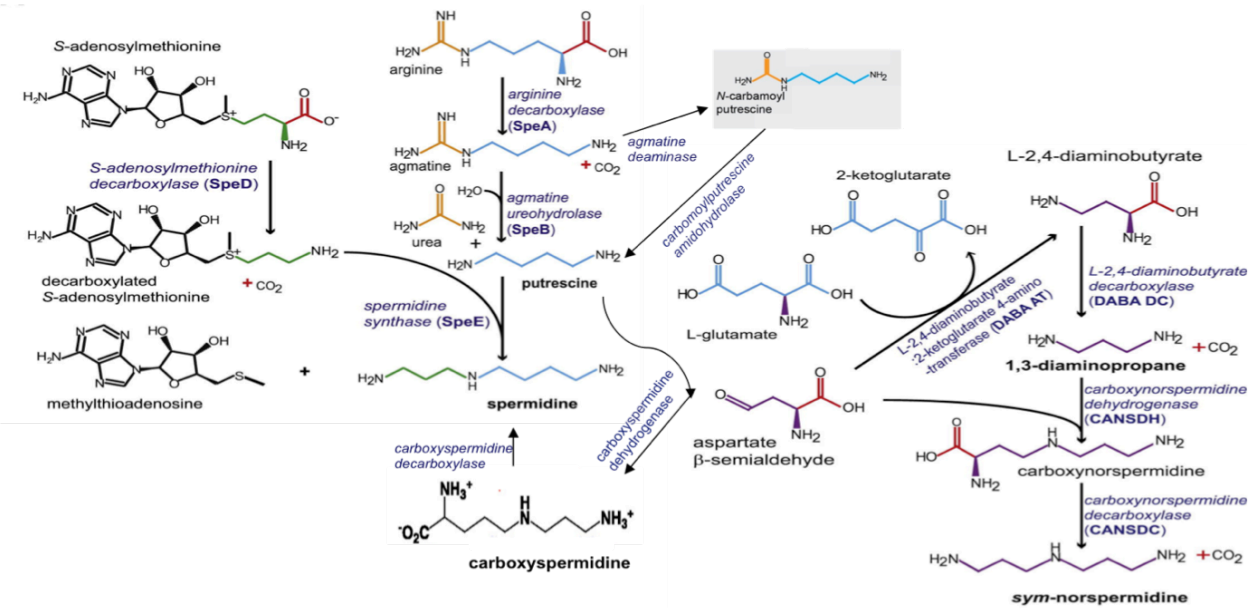

Figure 3. Polyamine biosynthesis pathways in bacteria. Modified from Hobley et al. 2014 and Lee et al. 2009.

Polyamine transport

To date, the majority of research on prokaryotic polyamine systems has been conducted using *Escherichia coli*. Putrescine is the most abundant intracellular polyamine in *E. coli,* followed by spermidine and cadaverine (43, 101). *E. coli* has two polyamine importers that are members of the ABC-type transporter superfamily. These are known as PotABCD and PotFGHI. ABC-type exporters are highly conserved and have been found in both eukaryotes and prokaryotes; however, ABC-type transporters that function in substrate uptake have only been identified in prokaryotes. As shown in Figure 4, this type of importer consists of a pair of cytoplasmic ATPases, two channel-forming transmembrane proteins, and a periplasmic substrate binding protein (64). The substrate is delivered to the inner membrane complex by the substrate binding protein, and deposited within the channel following interaction of the substrate binding protein with the transmembrane proteins. Subsequent hydrolysis of ATP within the nucleotide binding domain of the cytoplasmic ATPase results in a conformational change of the

transmembrane proteins, from outward- to inward-facing, allowing delivery of the substrate into the cell cytoplasm (64). This cycle typically requires the hydrolysis of two molecules of ATP (100).

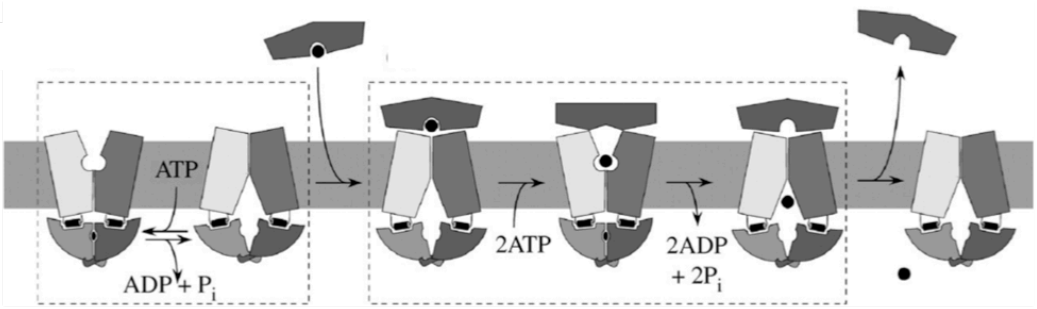

Figure 4. Mechanism of ATP-binding cassette type transporters. ABC-type transporters consist of a pair of cytoplasmic ATPases, two transmembrane permease proteins, and a periplasmic substrate binding protein. Energy from ATP hydrolysis by ATPases as well as interaction between the substrate binding proteins and transmembrane permeases is essential for functional transport. Modified from Locher 2009.

PotABCD is a spermidine-preferential ABC-type importer. It is also capable of putrescine import, though with much lower affinity. PotA is the cytoplasmic ATPase of this system, which hydrolyzes ATP to ADP, providing the energy essential to drive transport (30, 52, 54). PotB and PotC proteins each have six transmembrane-spanning segments, and form a channel through the inner membrane that substrates may pass through (30, 40). PotD is the periplasmic substrate binding protein, which binds either spermidine or putrescine and then interacts with the transmembrane domains to deliver the attached ligand (30, 46, 54, 55). PotD has a much higher affinity for spermidine than for putrescine; the K_d= 3.2 μM for spermidine, and K_d= 100 μM for putrescine. Likewise, uptake activity by the system is much higher for spermidine (Km=0.1 μM) than for putrescine (Km= 1.5 μM) (30, 43, 55). Uptake of polyamines by PotABCD is dependent on both ATP hydrolysis and membrane potential. Spermidine uptake was decreased by about 60% in the presence of of carbonyl cyanide m-chlorophenylhydrazone,

which disrupts membrane potential, indicating that optimal importer function is not achieved by ATP hydrolysis alone (54).

A number of regulatory roles have also been shown for the proteins of the PotABCD system. PotA contains a spermidine-binding site within the COOH-terminal domain. Excess spermidine within the cell may bind to this site, resulting in noncompetitive inhibition of ATPase activity, and subsequently, inhibition of transporter function (53). In wildtype *E.coli*, PotD is found in the periplasm, but in PotD-overexpressing strains, the full PotD protein can be found in the cell cytoplasm. In this case, PotD has been shown to act as a negative regulator of the *potABCD* operon, and can bind to the upstream region and inhibit transcriptional activation. This inhibitory effect is increased in the presence of spermidine. Other components of the system are incapable of eliciting this inhibitory effect (3). Whether an amount of PotD protein sufficient to generate this feedback response exists in the cytoplasm under wildtype expression levels has yet to be determined.

Effects of polyamines on biofilm formation

The role of polyamines in biofilm formation is just starting to be investigated in many species. Polyamines have been found to regulate biofilm formation in a variety of microbes, from human pathogens to non-pathogenic, environmentally found bacteria. A role of polyamines in biofilm formation has been shown in species including *E. coli, Yersinia pestis, Neisseria gonorrhoeae,* and *Vibrio cholerae.*

Spermidine and norspermidine, both triamines, have negative effects on biofilm formation in *E. coli*, while the diamine putrescine has a stimulatory effect (77, 94). Putrescine may stimulate biofilm formation through translational regulation of the response regulators UvrY

and CpxR (94). UvrY serves as a response regulator with a role of regulation of a variety of phenotypes including biofilm formation through modulation of small noncoding regulatory RNAs (62, 74, 84, 91, 118). CpxR is the response regulator for the sensor kinase CpxA, and this pair is involved in regulation of gene expression under copper-induced stress. They also repress biofilm formation in *E. coli* (78, 121, 122). The upstream region of *uvrY* mRNA contains an inefficient initiation codon. Replacement of the inefficient codon UUG with an efficient codon AUG resulted in decreased stimulation by polyamines. Similarly, the Shine-Dalgarno sequence of *cpxR* is located 10 nucleotides upstream from the initiation codon. Substitution of a S-D sequence at the ideal 7 nucleotides upstream decreased stimulation of gene transcription by putrescine. This indicates that polyamine regulation of CpxR and UvrY occurs at the level of translation, and that the increased translation of CpxR and UvrY in response to polyamine stimulation then modulates biofilm formation in *E. coli*, rather than polyamines more directly modulating the biofilm phenotype (94). It is worth noting, however, that wild-type *E. coli* cells grown in culture may contain 10-30 mM of putrescine, so whether these physiological effects can be solely attributed to the increased availability of putrescine at the relatively low concentration used in this study (0.6 mM) has yet to be determined (17, 101).

Y. pestis, the causative agent of the bubonic and pneumonic plague, required putrescine for biofilm formation (83). *Y. pestis* forms biofilms in the proventriculus of the flea host, and thus biofilms may be an important factor in plague transmission to humans (23, 49). Evidence suggests that putrescine modulates expression of *hms* genes, which are essential to biofilm formation (119). HmsT is located in the inner membrane and contains a conserved GGDEF domain, which indicates a function as a diguanylate cyclase, involved in production of c-di-GMP. Accordingly, HmsT acts as a positive regulator of *Y. pestis* biofilm formation (50, 56,

103). HmsP is an inner membrane protein with both GGDEF and EAL domains, indicating the potential for both diguanylate cyclase activity (c-di-GMP synthesis) and phosphodiesterase activity (c-di-GMP degradation.) At this point, only phosphodiesterase activity by HmsP has been confirmed, and HmsP negatively effects biofilm formation (8). HmsR and HmsS are both predicted inner membrane proteins thought to to be involved in polysaccharide production due to homology to *E. coli* PgaC and PgaD, respectively, which are both involved in synthesis of the surface polysaccharide poly-N-acetylglucosamine (PNAG) (15, 48, 63, 85).

Production of HmsR, HmsS and HmsT is dependent on polyamine accessibility, and protein levels decrease by 93%, 43%, and 90% respectively in the absence of polyamines (119). As depicted in Figure 5, both *hmsT* and *hmsR* lack an upstream consensus Shine-Dalgarno sequence, which is characteristic of genes that are modulated by polyamines (45, 126). Insertion of a consensus Shine-Dalgarno sequence upstream of *hmsT* resulted in a reduction of putrescine stimulation of translation by ~18%, indicating that biofilm formation is modulated by polyamines through translational regulatory mechanisms. Furthermore, *Y. pestis* mutants incapable of synthesizing putrescine were severely attenuated in the mouse model, suggesting a role for putrescine-dependent biofilm formation in *Y. pestis* virulence (119).

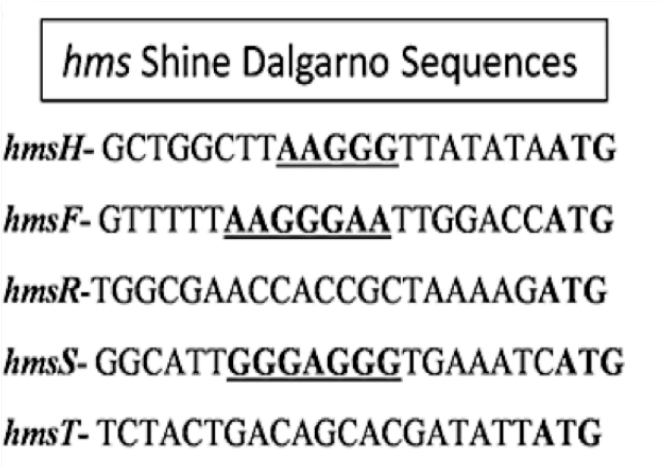

Figure 5. Shine-Dalgarno sequences of *Y. pestis hms* genes. Upstream sequences of each *hms* gene start codon. Consensus S-D sequences are underlined in *hmsH, hmsF,* and *hmsS*, while *hmsR* and *hmsT* lack consensus S-D sequences.

N. gonorrhoeae is a sexually transmitted obligate human pathogen that forms biofilms on human genital epithelial cells, indicating a role for biofilm formation in pathogenesis and survival in the human host (35). Polyamines may be present at concentrations ranging from 1-15 mM in the human urogenital tract, and therefore are likely encountered by the bacterium during infection (113). Furthermore, polyamines including spermine and spermidine have been shown to bind to the surface of gonococcal cells and increase survival in response to some antimicrobial peptides, suggesting that the availability of polyamines in the host urogenital tract may affect *N. gonorrhoeae* pathogenesis and virulence (35). Addition of spermine was shown to significantly reduce *N. gonorrhoeae* biofilm formation at a concentration as low as 0.5 μM, while a concentration of 4 μM of spermidine was required for a similar reduction (34). Although the mechanism through which spermidine and spermine inhibit biofilm formation has not yet been elucidated, it has been proposed that decreased biofilm formation in response to polyamines may improve spreading along the lining of the human urogenital tract during *N. gonorrhoeae* infection.

V. cholerae, the causative agent of the deadly diarrheal disease cholera, is also an extremely successful colonizer of aquatic environments including brackish waters and estuaries (19). It is nearly impossible to eradicate *V. cholerae* from aquatic environments following an outbreak, and the resulting endemicity poses a health hazard to human inhabitants, who may unintentionally ingest food or water contaminated with *V. cholerae* (18). Growth in a biofilm has been implicated in survival of *V. cholerae* in the native aquatic environment as well as within the human host, as it may provide protection against harsh environmental conditions as well as stomach and bile acids and increase virulence (42, 110). Polyamines including spermidine, spermine, putrescine, and cadaverine, are present in the human intestine, the exclusive location of *V. cholerae* colonization in the human host, suggesting a potential interaction between this bacterium and these molecules during infection (4). Polyamines in the intestine may originate from the human diet, which is thought to contain hundreds of micromoles of polyamines such as spermidine, putrescine, and spermine. Intestinal polyamines may also be contributed by gut microbiota, or by intestinal cells, which are capable of synthesizing and exporting polyamines (66, 73, 75). Polyamines are present in the human intestinal lumen. Spermidine, for example, is present at approximately 100 μM in bile and duodenal fluids (67, 81). Because the biofilm phenotype may be an essential factor to survival in both the environment and within the host, *V. cholerae* serves as a useful model organism through which to study regulation of biofilm formation by polyamines.

Polyamines have been demonstrated to effect *V. cholerae* biofilm formation through both extracellular and intracellular mechanisms. The NspS-MbaA sensory system modulates biofilm formation in response to extracellular polyamines. Deletion of *nspS* results in reduced biofilm formation, indicating that NspS stimulates biofilm formation. In contrast, deletion of *mbaA*

enhances *V. cholerae* biofilm formation, indicating that *mbaA* represses biofilm formation (51, 117). Vibriopolysaccharide (VPS) is produced by *V. cholerae* cells within a biofilm, and is an essential extracellular matrix component. VPS production is dependent on expression of *vps* genes, which are arranged in two operons, *vpsA-K,* and *vpsL-Q*, both of which are under the control of the response regulators VpsR and VpsT (11, 117, 125). Development of robust biofilms in the Δ*mbaA* mutant was dependent on production of VPS, indicating that MbaA plays a role in biofilm maturation through a VPS-dependent mechanism (9). Further investigation into the function of *mbaA* identified conserved GGDEF and EAL domains, indicating a potential role as a regulator of c-di-GMP (9). As stated previously, GGDEF domains are highly conserved among enzymes with diguanylate cyclase activity, which generates c-di-GMP. Conversely, EAL domains are found in enzymes with phosphodiesterase activity, which are involved in degradation of c-di-GMP (31). Purified C-terminal MbaA demonstrates c-di-GMP phosphodiesterase activity, and is capable of degrading c-di-GMP into pGpG, suggesting that the action of MbaA in reducing intracellular levels of c-di-GMP is what controls the effects seen on biofilm formation (16).

Originally annotated as the ligand-binding protein of a polyamine transporter, NspS was shown to enhance biofilm formation in the presence of norspermidine, but not spermidine. Furthermore, this effect was dependent on *mbaA*, and addition of norspermidine to *ΔmbaA* strains had no effect on biofilm formation (51). The NspS-MbaA interaction appears to alter biofilm formation in a VPS-dependent manner, and *vpsL* transcription in *ΔmbaA* strains was twice the level observed in wildtype, as demonstrated through a β-galactosidase assay of *V. cholerae* strains harboring a chromosomal *vpsLp-lacZ* promoter fusion. Transcription of *vpsL* was also increased by almost two-fold in the wild-type strain in the presence of norspermidine

(51). The current model of the NspS-MbaA interaction and role on biofilm formation is illustrated in Figure 6. Taken together, this information suggests that MbaA acts as a repressor of biofilm formation, and NspS acts to prevent this repression in the presence of norspermidine.

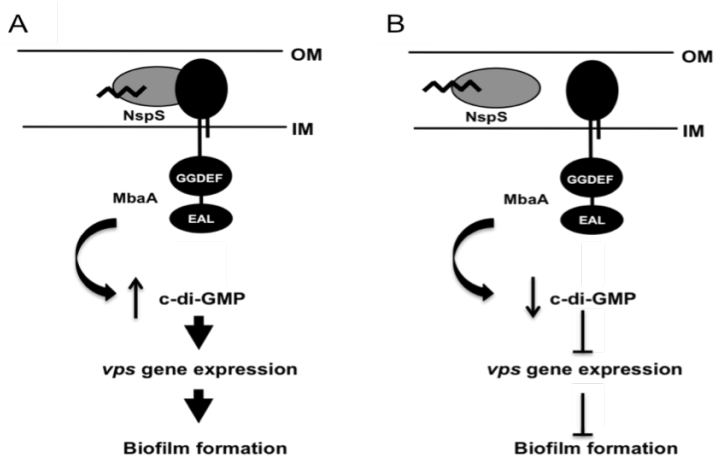

Figure 6. Predicted mechanism of NspS-MbaA interaction and effects on *V. cholerae* biofilm formation. (A) NspS bound to norspermidine interacts with MbaA and prevents phosphodiesterase activity leading to an increase in c-di-GMP, *vps* gene expression, and biofilm formation. (B) NspS bound to spermidine cannot interact with MbaA, which degrades c-di-GMP through phosphodiesterase activity, leading to reduced *vps* gene expression and decreased biofilm formation. Modified from Cockerell, *et al* 2014.

Polyamines may also modulate *V. cholerae* biofilm formation through intracellular mechanisms. In addition to the common polyamines putrescine, spermidine, and cadaverine, species of *Vibrio* also have high levels of intracellular norspermidine, and rarely contain detectable levels of spermine. Vibrio was the first mesophilic genera found to contain norspermidine, which was previously associated with thermophilic bacteria (117, 124). Some polyamines, including norspermidine, may be synthesized *de novo,* or may be imported from the surrounding environment. Predicted biosynthesis pathways are shown in Figure 3.

Norspermidine synthesis is dependent on two enzymes: carboxynorspermidine dehydrogenase (CANSDH) which synthesizes the intermediate carboxynorspermidine from diaminopropane and aspartate β-semialdehyde, as well as carboxynorspermidine decarboxylase (CANSDC) which generates norspermidine through the decarboxylation of

carboxynorspermidine (76, 108, 123). Both CANSDH and CANSDC are essential to *V. cholerae* biofilm formation, and defects in biofilm formation in response to disruption of either gene could be alleviated by addition of exogenous norspermidine to biofilm growth media, suggesting an essential requirement for norspermidine in *V. cholerae* biofilm formation (59). Overexpression of the *V. cholerae* CANSDC gene, *nspC*, led to increased growth rate and reduced lag time in shaking liquid culture. Similarly, biofilm cell density was five-fold higher in strains overexpressing *nspC* compared to wildtype. This was shown to be VPS-dependent using the previously described β-galactosidase assay and strains with a chromosomal *vpsLp-lacZ* fusion, suggesting that intracellular norspermidine influences biofilm formation through a VPS-dependent, but yet unknown mechanism (82). Interestingly, overexpression of CANSDC does not lead to an increase in levels of norspermidine within the cell or in spent medium, suggesting that optimal levels of norspermidine are maintained within the cell through a yet unidentified mechanism (82).

The *V. cholerae* genome encodes an ABC-type polyamine transporter, *potABCD2D1,* which is homologous to the *potABCD* operon in *E. coli*, depicted in Figure 7. As in the *E. coli* transporter, PotA is annotated as the ATPase, and PotB and PotC are annotated as the transmembrane permeases. Interestingly, this system is annotated with two substrate-binding proteins, referred to as PotD2 and PotD1. However, at this point, only PotD1 has been shown to have a role in polyamine uptake (16, 68). The predicted proteins encoded by genes in this putative operon have 59-72% amino acid sequence identity to PotABCD in *E. coli* (68). While the PotABCD system is responsible for uptake of spermidine and putrescine in *E. coli,* the *V. cholerae* PotD1 is involved in the uptake of both spermidine and norspermidine. As such, PotABCD2D1 as the first norspermidine transporter discovered in any species (16, 68). Previous

research has demonstrated an essential role for PotB and PotC, the transmembrane channel-forming proteins, in uptake of both spermidine and norspermidine (96). The role of PotA, the putative ATPase of this system, is still under investigation, and is the subject of the work presented here. Confirmation of involvement of PotA is essential to determine if the entire system functioning as a whole is what elicits the effects seen on biofilm formation, rather than one or more of the involved genes having a more direct role.

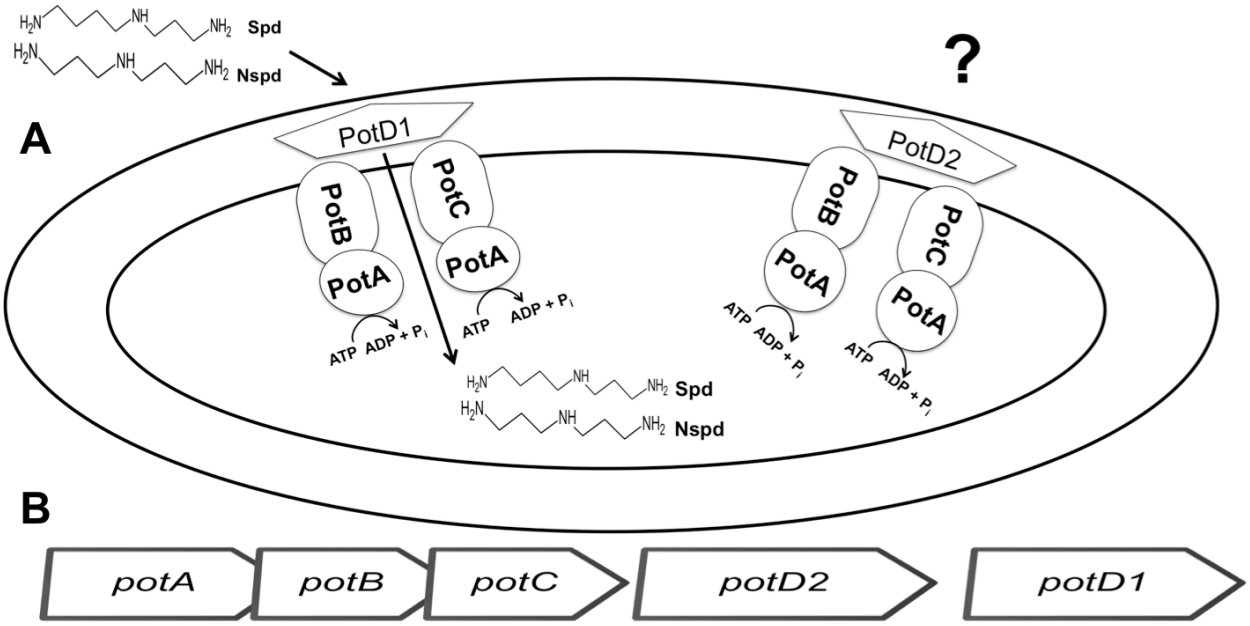

Figure 7. Schematic of PotABCD2D1 in *V. cholerae*. (A) Depiction of the ABC-type transporter complex. The substrate binding proteins, PotD1 and PotD2 are located in the periplasm, the transmembrane proteins PotB and PotC form a pore through the inner membrane, and the ATPase PotA is located in the cytoplasm. (B) Organization of the putative *pot* operon.

V. cholerae virulence

A hyperinfectious phenotype is exhibited by *V. cholerae* grown in a biofilm, suggesting a role for biofilm-promoting genes in association of *V. cholerae* with other organisms (110). While over 200 serotypes of *V. cholerae* have been identified, only two are associated with the

disease cholera. These are the O1 serotype of both El Tor and Classical biotype, and the O139 serotype. The pathogenic nature of these strains is dependent on several virulence factors, including cholera toxin, toxin coregulated pili (TCP), and the accessory colonization factors (39).

Cholera toxin is the essential toxin for manifestation of the disease cholera. Cell free, purified "cholerigenous factors" containing cholera toxin are sufficient to induce cholera symptoms in human volunteers (6). The toxin is an 84-kD protein made up of a single A subunit and five B subunits arranged in a pentameric ring and encoded by the *ctx* genes (95, 128). The B subunits are involved in host cell recognition and attachment, following which the entire toxin is endocytosed (61). Following entry into the cell, the A subunit ADP-ribosylates Gs alpha subunit ($G\alpha_s$) proteins on the host cell surface, preventing GTPase activity and resulting in constitutive activation of $G\alpha_s$. The activated G protein over-stimulates adenylate cyclase activity, leading to excess cAMP production (12, 33). Presence of elevated cAMP leads to activation of PKA, which then phosphorylates serine residues in the regulatory region of cystic fibrosis transmembrane conductance regulator (CFTR) proteins, leading to disruption of transmembrane channel regulation and leading to excessive secretion of Cl^- into the intestinal lumen, as well as reduced import of Na^+ (13, 105). This disruption of ion balance and subsequent water loss from the intestinal epithelial cells results in the severe dehydration and watery diarrhea, or "rice-water stool" characteristic of this disease. The genes for cholera toxin are encoded on a CTX genetic element acquired from a filamentous bacteriophage and integrated in to the *V. cholerae* chromosome. Disruption of the gene encoding the A subunit, *ctxA*, substantially attenuates cholera symptoms but does not significantly alter colonization ability in the human intestine, suggesting that cholera toxin is not involved in colonization but rather in producing the characteristic severe diarrheal response (39).

Toxin-coregulated pili (TCP) are required for attachment and colonization of intestinal epithelial cells in the intestine and are made up of a single subunit, TcpA (39, 111). These type IV pili are necessary for cell-cell adhesion among bacteria, allowing development of microcolonies essential for colonization during the course of infection (14, 57, 109, 111). TCP also serve as the receptor for the CTX bacteriophage carrying the necessary genes for cholera toxin, and TCP-deficient strains cause no symptoms of cholera and are incapable of colonizing the human intestine (115).

Motility and chemotaxis are thought to be important processes in the progression of *V. cholerae* colonization and subsequent infection, primarily based on *in vitro* assays. Mutations causing alterations in motility phenotypes may be linked to altered TCP expression. Nonmotile mutants have demonstrated increased TCP and cholera toxin production, and increased motility may correlate inversely with production of TCP and cholera toxin (32). Virulence factor expression is controlled by the master regulator ToxT (37, 98). This suggests integral regulation between motility and virulence factor expression in order for colonization to progress. It would be expected that chemotaxis, directional movement of a bacterium towards a favorable stimulus or away from an unfavorable stimulus, would be beneficial to motility and colonization in the host. However, *V. cholerae* shed from the human intestine typically demonstrate reduced chemotaxis gene expression. Furthermore, chemotaxis-deficient, motile strains of *V. cholerae* have increased infectivity compared to strains exhibiting chemotaxis capabilities, and a reduced inoculum is required in order to generate infection symptoms (10).

Expression of virulence factors including cholera toxin, TCP, and other accessory factors by *V. cholerae* within the host is highly regulated and controlled by a cascade of effectors. A brief outline is shown in Figure 8.

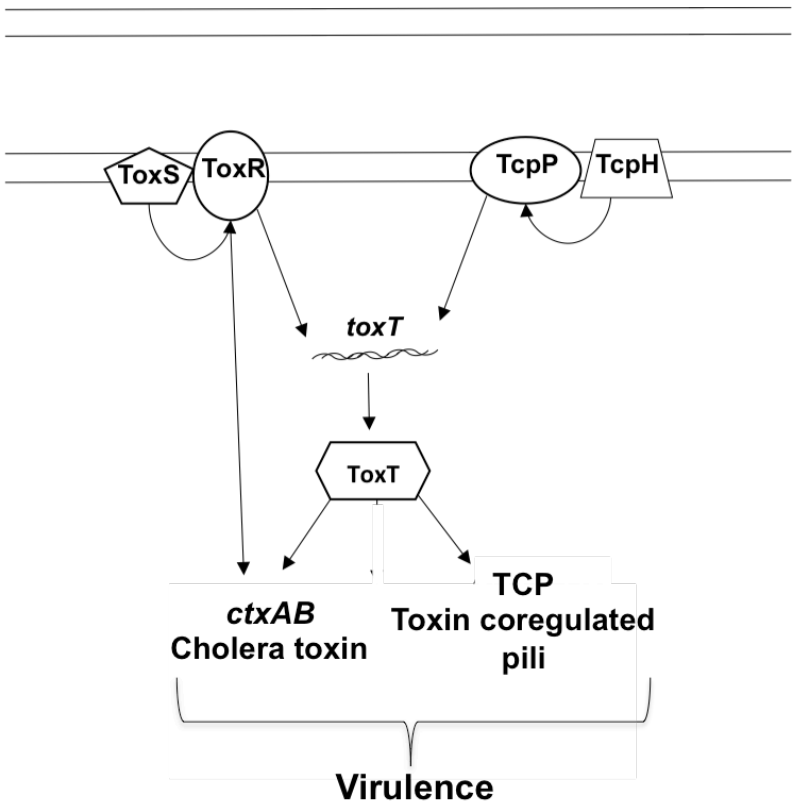

Figure 8. Current model of virulence cascade in *V. cholerae*. ToxS-ToxR interaction at the membrane increases activity of ToxR. TcpP is also activated at the membrane by TcpH. TcpP and ToxR both independently activate ToxT, which regulates expression a variety of colonization and virulence factors including *ctxA* and *tcpA*. Illustrated using Microsoft PowerPoint.

Animal models for cholera

To date, mammalian models have primarily been used to study the association and pathogenesis of cholera-causing *V. cholerae* with other organisms. At this point, humans are the only known adult mammalian host that can be naturally colonized by *V. cholerae*, so significant manipulations to the animal are often necessary in order to facilitate and maintain colonization in other adult mammals. Suckling mammals may be colonized through intragastric or orogastric inoculation. This increased susceptibility is potentially due to an underdeveloped immune system and/or commensal microbial population (89). Mice and rabbits have been the most commonly used animal models for the study of *V. cholerae*. Nonmammalian models have been

developed more recently. Both arthropods and fish may associate with *V. cholerae* in the natural environment, which has led to the investigation of the capabilities of *V. cholerae* to colonize and/or infect the well-established model organisms *Drosophila melanogaster* and *Danio rerio* (zebrafish) (7, 92, 99, 102). Colonization can be achieved in both *D. melanogaster* and zebrafish simply through ingestion of the bacterium, with no additional measures necessary to maintain colonization. Each model provides a unique set of benefits and drawbacks in the study of the disease cholera.

Successful colonization of adult mice resulting from oral inoculation is dependent on treatment with the anesthetic xylazine as well as sodium bicarbonate in order to neutralize stomach acid (79, 80). *V. cholerae* colonizes the crypts of the distal small intestine in a TCP-independent manner, and cholera toxin has only a small effect on disease progression in the adult mouse (80). For the most part, the mechanism of *V. cholerae* infection of adult mice does not resemble infection in humans; however, adult mice have provided some insight into accessory colonization factors.

The infant mouse is, to date, the most frequently used model organism in the study of *V. cholerae* infection. Suckling infant mice are typically intragastrically inoculated at 3 to 5 days of age. Many of the same virulence genes that are essential in human infection are highly expressed by *V. cholerae* in the mouse intestine (28, 111). As in human infection, TCP are required for colonization of the mouse intestine, and the middle region of the small intestine is preferentially colonized (2, 111). Whether this is in response to recognition of similar host cell receptors in both the mouse and human, or simply due to the amount of time required by the bacteria to adapt to environmental surroundings in order to colonize is not known. Likewise, mice fed purified cholera toxin produce increased levels of intestinal fluid, similar to the human

response to cholera toxin (5). TCP are essential for colonization of the small intestine, but colonization of the large intestine is TCP-independent (2, 111). Whether a similar colonization of the large intestine occurs in humans has not been determined. Cholera toxin-deficient strains demonstrate reduced lethality to mice, but colonization levels are not significantly affected, supporting the role of cholera toxin in pathogenesis but not colonization. However, infant mice are removed from their mothers in order to perform infection experiments, so survival time is relatively short, typically 2-3 days after isolation. As such, it is difficult to monitor lethality of the disease in this model (58).

Inconsistencies have arisen in the study of motility in the infant mouse intestine. Under some conditions, aflagellate and flagellated motility-deficient mutants show little disadvantage in colonization of the infant mouse intestine compared to wildtype. It has been hypothesized that the mucus layers of the infant mouse may differ from the adult rabbit, which may facilitate colonization by nonmotile strains (88). However, other studies have reported severe attenuation of both aflagellated and flagellated nonmotile mutants (60). Thus, the role of motility in colonization of the infant mouse intestine has yet to be determined. Nonchemotactic, motile mutants demonstrated increased colonization and altered distribution in the infant mouse intestine. While the distal small intestine is preferentially colonized by wild-type *V. cholerae*, non-chemotactic *V. cholerae* uniformly colonizes both the small intestine and stomach (60). Therefore, chemotaxis may inhibit *V. cholerae* colonization of the infant mouse intestine.

Biofilm affords a colonization advantage to *V. cholerae* in the infant mouse intestine, as *V. cholerae* cells inoculated while biofilm-bound are capable of achieving levels of colonization 5.8-fold higher than when inoculated in the planktonic cell form. This colonization advantage is maintained even when biofilms are dispersed prior to inoculation of mice, indicating that the

physiological state of cells within the biofilm themselves imparts the colonization advantage, rather than mechanical protection provided by the biofilm structure (110). This colonization advantage is apparent as little as 5 hours after inoculation, and may be maintained up to 24 hours. Thus, the infant mouse has provided much insight into *V. cholerae* colonization and virulence factors that can be applied to pathogenesis in humans.

Adult rabbits have been utilized as models to study *V. cholerae* for over 60 years (24). Adult rabbits require surgical manipulations in order to achieve and maintain colonization and infection of the small intestine by mechanically preventing clearing of bacteria from the intestine (72). Known human virulence factors *tcpP, tcpH,* and *toxR* are transcribed at high levels in the rabbit intestine, implying a role for these genes in rabbit colonization as well (120). *V. cholerae* strains deficient in TCP and cholera toxin production do not cause diarrhea in adult rabbits, and strains lacking TCP were only shed from the rabbit intestine for two days, as opposed to shedding of wild-type throughout the entire week-long observation period, indicating deficient or nonexistent colonization by TCP-deficient strains (26). Additionally, nonmotile mutants, whether aflagellated or flagellated, demonstrated a colonization defect in comparison to motile parent strains, indicating that motility is an important colonization factor in the adult rabbit intestine (88). Thus, the adult rabbit model may be useful for studying some colonization factors that are essential in human infection.

Trials using the infant rabbit as a model to study cholera began as early as 1894, but initial experiments involving oral inoculation of infant rabbits failed to generate consistent symptoms or results (25, 70). It has since been determined that establishment of cholera disease through orogastric inoculation of infant rabbits is dependent on pretreatment with cimetidine, which reduces stomach acidity (90, 97). While rabbit models require manipulation through

surgical or pretreatment means, infection, if achieved, has many similar characteristics to human cholera. Rabbits develop severe, watery diarrhea that is similar to the characteristic rice-water stool of human cholera infection, and this may lead to severe weight loss (90, 93, 104). Similar to human illness, development of diarrhea and dehydration is also dependent on toxin production in the rabbit, and strains of *V. cholerae* that do not produce cholera toxin demonstrate reduced virulence in infant rabbits (90, 104). Likewise, mutants that do not produce TCP do not cause significant disease in the infant rabbit; however, these mutants are capable of colonizing, which leads to development of increased cecal fluid accumulation (90). Thus, many virulence factors and symptoms of *V. cholerae* in infant rabbits parallel *V. cholerae* infection in humans (39, 107).

As an aquatic organism, *V. cholerae* is often found associated with aquatic arthropods in the natural environment, presumably through insect consumption of water contaminated with *V. cholerae* (102). Thus, use of an arthropod model for *V. cholerae* study is a logical choice. *V. cholerae* is capable of survival and proliferation within *D. melanogaster* following ingestion of the bacterium delivered through the fly food. As in humans, the intestine is the specific site of *V. cholerae* colonization within *D. melanogaster.* As the disease develops in the fly, significant and weight loss may occur, leading to death. This parallels the symptoms of human patients with severe cases of cholera. Weight loss and death are dependent on production of cholera toxin; however, unlike in human cases, cholera toxin alone is not lethal to the flies. Inoculation of purified cholera toxin and a *V. cholerae* strain deficient in cholera toxin production restores lethality. Therefore, some additional factor produced by *V. cholerae* is required for cholera toxin activity in *D. melanogaster* that has not been identified in other models. Manifestation of symptoms depends on $G_{s\alpha}$ and adenylyl cyclase activity, indicating a similar mechanism of disease in *D. melanogaster* and humans (7).

Several studies have demonstrated a role for biofilm formation in colonization of the *D. melanogaster* intestine by *V. cholerae.* *vps* gene transcription is highly upregulated in *V. cholerae* in the fly intestine, and mutants unable to synthesize VPS demonstrate a colonization defect compared to wild-type. *V. cholerae* strains that are unable to produce VPS are incapable of colonizing the rectum of *D. melanogaster*, while wild-type strains typically coat the epithelial surface of this region. As *V. cholerae* is retained in the rectal pouch following clearing of the small intestine in surviving *D. melanogaster*, adhesion in this region may be crucial for dispersal and transmission following infection (86). Proteins Bap1 and RbmC are essential for attachment and stabilization of *V. cholerae* biofilms, and Δ*bap1*Δ*rbmC* strains are also significantly impaired in colonization of the *D. melanogaster* intestine (1). Taken together, this data suggests a potential role for *V. cholerae* biofilm formation in *D. melanogaster* colonization.

V. cholerae can also be found associated with aquatic organisms including fish, so a well-studied model organism such as the zebrafish presents a logical model through which to study *V. cholerae* colonization and infection ability. Fish may provide a means of transmission and dispersal for *V. cholerae* in the aquatic environment (99). Recent studies have demonstrated that pathogenic strains of *V. cholerae* O1 are capable of specifically colonizing the intestine of both the adult and larval zebrafish following addition of bacterial cultures to the fish tank water, and that this colonization can be achieved in as little as two hours after exposure. Colonization is not lethal to the fish, and *V. cholerae* can be transmitted from uninfected fish to naïve fish. A *toxT* mutant, which does not produce TCP, cholera toxin, or other accessory factors shown to be essential for colonization and infection in humans and other animal models, colonized as well as wild-type *V. cholerae*, indicating that the essential virulence factors in human infection are not

required for colonization of the fish (92). As the zebrafish is a relatively new model for *V. cholerae* study, essential colonization factors have not yet been determined.

Purpose of this study

The goals of the current study were twofold. First, I aimed to determine the role of PotA in uptake of norspermidine and spermidine through the novel ABC-type transporter PotABCD1, and subsequently observe effects on biofilm formation. The second aim was to investigate the role of genes that act as biofilm regulators in response to polyamine levels in fish colonization in order to elucidate essential factors to this association. This study provided more information on ABC-type transporters, an extremely well conserved protein family. Additionally, the results generated from this study provided further insight into polyamine regulation of biofilm formation. This provided further evidence of the importance of polyamines and biofilm formation in *V. cholerae* environmental and host survival, as well as information about a potential novel environmental reservoir of *V. cholerae.*

Materials and Methods

Bacterial strains and growth conditions

Bacterial strains are listed in Table 1, plasmids are listed in Table 2, and primers are listed in Table 3. Primer synthesis and sequencing was performed by Eurofins, MWG (Huntsville, AL.) All strains were grown in Luria-Bertani (LB) or tryptone broth. LB broth is composed of 1% Tryptone, 0.5% Yeast Extract, and 85mM NaCl. Tryptone broth is composed of 1% Tryptone and 85mM NaCl. When required, antibiotics were added to growth media at the following concentrations: ampicillin, 100 μg/mL; streptomycin, 100 μg/mL; tetracycline, 2.5 μg/mL. Plasmids were extracted and purified using Promega Wizard Plus SV Minipreps DNA Purification System (Madison, WI.) Polyamines including putrescine dihydrochloride (putrescine), 1,3-diaminopropane dihydrochloride (diaminopropane), cadaverine dihydrochloride (cadaverine), bis(3-aminopropyl)amine (norspermidine), and spermidine trihydrochloride (spermidine) were obtained from Sigma (St. Louis, MO). Restriction enzymes, Calf intestinal alkaline phosphatase (CIP), and Phusion and OneTaq polymerases were obtained from New England Biolabs (Beverly, MA).

Deletion of V. cholerae potA gene

Primers were generated to amplify regions of approximately 400 bp upstream and downstream from the *potA* gene. PA242 was designed to anneal to the nucleotide 301 base pairs upstream from the *potA* start codon, and PA243 was designed to anneal to the nucleotide 144 base pairs downstream from the *potA* start codon. PA244 was designed to anneal to the nucleotide 71 base pairs upstream from the *potA* stop codon, and PA246 was designed to anneal to the nucleotide 234 base pairs downstream from the *potA* stop codon. These regions were

amplified through PCR with Phusion polymerase from New England Biolabs and purified using a GE Healthcare Illustra™ GFX™ PCR DNA and Gel Band Purification Kit (Buckinghamshire, UK). Upstream and downstream fragments were then added to a single reaction in order to allow complementary regions on internal primers PA243 and PA244 to re-anneal following denaturation, resulting in gene splicing by overlap extension (SOE) and generating an in-frame deletion of 918 base pairs (bp) of the total 1,133 bp in the *potA* gene (41). External primers PA242 and PA246 were added to this reaction in order to amplify the Δ*potA* fragment with Phusion polymerase. Presence of the 918 bp deletion fragment was verified by gel electrophoresis and the fragment was purified. The purified fragment was adenylated on the 3' ends, cloned into TOPO Vector pCR2.1 from Invitrogen (Carlsbad, CA) and electroporated into *E. coli* DH5α using a BIO-RAD MicroPulser (Hercules, CA) at 1.8 kv. Cells were recovered for 1 hour following electroporation in SO media (20 g/L tryptone, 5 g/L yeast extract, 0.548 g/L NaCl, 0.186 g/L KCl, 1 mM $MgCl_2$, 1 mM $MgSO_4$, and 2 mM glucose) at 37°C with shaking at 200 rpm, and then plated on LB agar containing 100 μg/mL ampicillin (Gold Biotechnology, Saint Louis, MO) and 20 μg/mL X-gal (20 mg 5-bromo-4-chloro-3-indolyl-β-d-galactopyranoside [Gold Biotechnology] in 1 mL dimethyl sulfoxide [ThermoFisher Scientific ™, Pierce™, Waltham, MA.])

Presence of the insert and correct fragment size was verified by PCR and gel electrophoresis, and then plasmids from positive colonies were selected for plasmid miniprep using Promega Promega Wizard Plus SV MiniPreps DNA Purification System (Madison, WI.) Plasmids sequenced for construct confirmation by Eurofins, MWG. The fragment was then excised from pCR2.1 using EcoR1 (New England Biolabs), purified, and ligated into pWM91 plasmid linearized with the same enzyme. The 5' ends of the pWM91 plasmid were

dephosphorylated using CIP in order to prevent recircularization of the plasmid prior to ligation of the insert. A schematic of this process is depicted in Figure 9.

The ligation was then electroporated into *E. coli* DH5α λ-pir. Plasmid uptake was verified by colony PCR. Colonies containing the correct-size insert were purified and electroporated into the conjugative strain *E. coli* SM10 λ-pir. Cells were recovered for 1 hour following electroporation in SOC medium as previously described, then plated on LB plates containing ampicillin and X-gal at 100 μg/mL and 20 μg/mL, respectively.

Following verification of plasmid uptake through colony PCR, the *E. coli* strain was conjugated with *V. cholerae* strain PW357 through SacB counter selectable mutagenesis in order to generate a chromosomal mutation in *potA* (69). PW357 contains a chromosomal *vpsLp-lacZ* promoter fusion inserted into the *V. cholerae lacZ* gene locus which allows measurement of β-galactosidase activity to quantify *vps* gene expression. (69). SacB counter selectable mutagenesis utilizes double homologous recombination with sucrose selection. Recipient and donor strains were mated by streaking on LB agar and incubated at 37°C overnight. One half of growth was streaked on each of two LB agar plates containing streptomycin at 100 μg/mL (Amresco, Solon, OH) and ampicillin at 50 μg/mL and incubated at 37 °C overnight. Four colonies were selected and purified by again streaking on selective agar containing streptomycin and ampicillin at 100 μg/mL and 50 μg/mL, respectively. The next day, four single colony isolates were streaked on LB with no antibiotic selection and incubated overnight at 37°C to allow a second recombination or "crossing out" event, resulting in removal of the ampicillin resistance encoded on the pWM91 plasmid and *sacB* gene. Isolated colonies were then streaked on 10% sucrose plates made by adding 5 g tryptone, 2.5 g yeast extract, and 7.5g agar to 333.5 mL diH_2O, autoclaving, than adding of 166.5 mL of filter-sterilized 30% sucrose solution

(Amresco). Finally, isolated colonies were patched on plates containing ampicillin (100 μg/mL) or streptomycin (100 μg/mL). Colonies resistant to streptomycin but sensitive to ampicillin were selected for colony PCR verification of *potA* deletion.

A similar protocol was followed in order to generate a Δ*potA* in the *nspC::kan* background with a few modifications. The *V. cholerae* genome contains *nspC,* which encodes carboxynorspermidine decarboxylase, the enzyme responsible for catalyzing the final step of norspermidine synthesis. In order to quantify only imported norspermidine, *nspC* was disrupted through insertion of a kanamycin resistance cassette in strain AK314A; therefore, AK314A was used as the recipient strain to generate the double mutant (16). Donor and recipient strains (AK420 and AK314A, respectively) were mated by streaking on LB agar and incubating at 37°C overnight. One half of the growth was streaked on one of two LB agar plates containing streptomycin at 100 μg/mL, ampicillin at 50 μg/mL, and kanamycin at 30 μg/mL (Amresco) and incubated at 37°C overnight. Four colonies were selected and purified by again streaking on selective agar containing the same concentrations of streptomycin, ampicillin and kanamycin. The next day, four single colony isolates were streaked on LB agar and with no antibiotic selection and incubated at 37°C overnight to allow a second recombination, "crossing out" event. Isolated colonies were streaked on 10% sucrose/kanamycin (30 μg/mL) plates and incubated at room temperature for two days. Isolated colonies were then patched on plates containing ampicillin (100 μg/mL) alone or streptomycin (100 μg/mL) and kanamycin (30 μg/mL). Colonies resistant to streptomycin and kanamycin but sensitive to ampicillin were selected for colony PCR to verify presence of Δ*potA*.

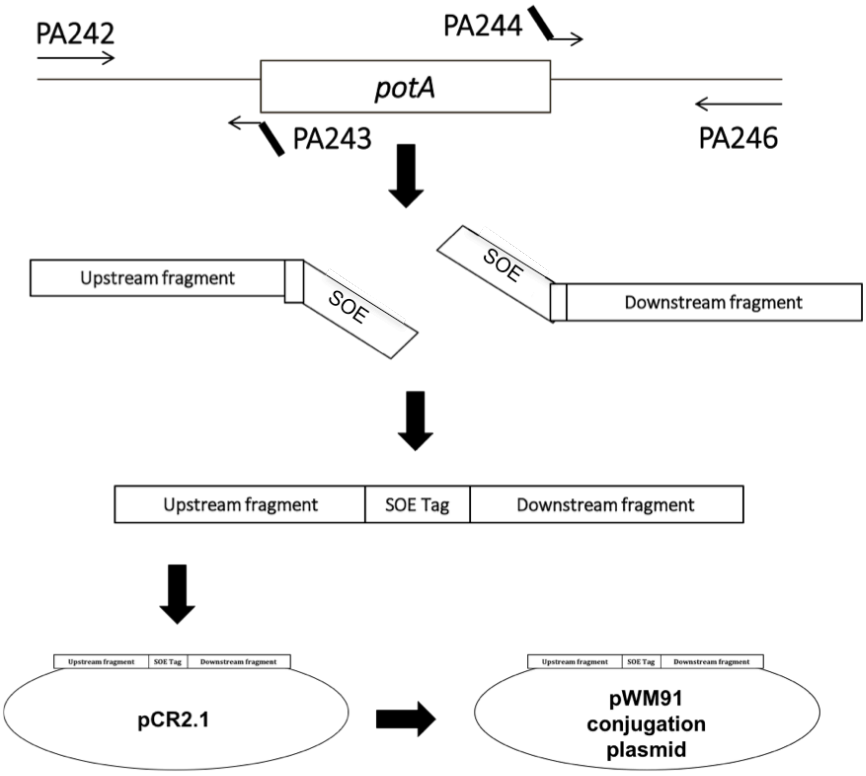

Figure 9. Construction of the pEV1 and pEV2 plasmids containing an in frame deletion of *potA*. Amplification of upstream and downstream fragments with complementary SOE tags facilitated removal of 918 of 1,133 base pairs of *potA*. This construct was cloned into pCR2.1 (pEV1), digested, and ligated into pWM91 conjugation plasmid (pEV2) for cross into *V. cholerae*.

Complementation of V. cholerae ΔpotA strain

In order to validate the requirement for PotA in spermidine and norspermidine uptake, Δ*potA* was complemented with *potA* on a plasmid. The entire *potA* gene was amplified from *V. cholerae* chromosomal DNA using primers PA251 and PA252, specific to the region 15 bp upstream of the predicted *potA* ribosome binding site and directly upstream from the *potA* stop codon. The forward primer contained an NcoI site directly upstream to the *potA* annealing region, while the reverse primer also encoded a V5 epitope tag, stop codon, and NcoI restriction site. These fragments were amplified with PA251 and PA252 using Phusion polymerase, cloned into TOPO Vector pCR2.1, and electroporated into *E. coli* DH5α. Cells were recovered and

plated as previously described. Correct insert fragment size was verified by colony PCR and gel electrophoresis in order to detect a fragment at the predicted 1,240 bp. Plasmids were extracted, purified, and sequenced for verification. Mutation of the NcoI site in the reverse primer was detected during sequencing. This was corrected by amplifying the 1240 bp fragment with PA251 and PA258, containing a corrected NcoI site, and then repeating the cloning, PCR, and sequencing procedure to verify correction of the NcoI site sequence.

The *potA-V5* fragment was then excised from pCR2.1 using NcoI restriction enzyme, ligated into pACYC184 linearized with the same enzyme and dephosphorylated as previously described, then electroporated into *Escherichia coli* DH5α. Plasmid uptake was verified by colony PCR, and plasmids were extracted and purified. Plasmids were then electroporated into *V. cholerae* mutant strains, and verified through colony PCR and gel electrophoresis. A schematic of this process is depicted in Figure 10.

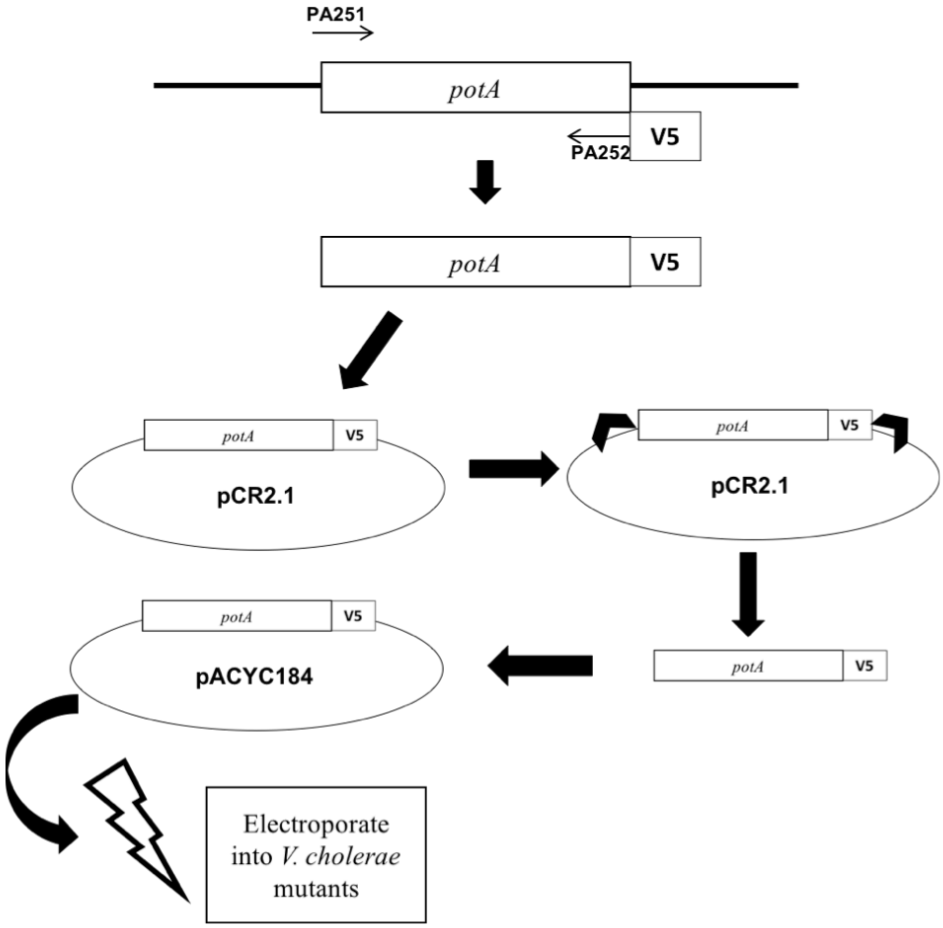

Figure 10. Construction of the pEV3 and pEV4 plasmids containing *potA-V5*. The entire *potA* gene was amplified. The reverse primer PA252 also encoded a V5 tag. This fragment was cloned into pCR2.1 (pEV3) digested, and ligated into pACYC184 (pEV4) for electroporation into *V. cholerae.*

Deletion of V. cholerae potD3 gene

Observation of spermidine uptake in the Δ*potD1* mutant, but not Δ*potA*, Δ*potB*, or Δ*potC,* when grown in the presence of high concentrations of spermidine, supporting previous identification of *VCA1113* as a possible *potD3* and low-affinity spermidine transporter (20). This led me to construct an in-frame deletion in this gene as previously described. Primers were constructed specific to regions upstream and downstream of the *potD3* gene. PA293 was designed to anneal 179 bp upstream from the *potD3* start codon, and PA294 was designed to anneal 207 bp downstream from the *potD3* start codon. PA295 was designed to anneal 149 bp

upstream from the *potD3* stop codon, and PA296 were designed to anneal 193 bp downstream from the *potD3* stop codon. Presence of PCR products at approximately 400 bp were verified by gel electrophoresis and gel purified. Fragments were combined in one reaction to allow re-annealing of complementary regions on PA294 and PA295 following denaturing, resulting in an in-frame deletion of 675 bp of the total 1,031 bp gene. PA293 and PA296 were added to this reaction along with Phusion polymerase in order to amplify the fused fragment. Fusion was verified by the presence of a product at approximately 778 bp visualized through gel electrophoresis. The PCR fragment, adenylated on the 3' ends, cloned into TOPO Vector pCR2.1, and electroporated into *E. coli* DH5α. Cells were recovered for 1 hour following electroporation in SOC media at 37°C with shaking at 200 rpm, and then plated on LB agar containing 100 μg/mL ampicillin and 20 μg/mL X-gal. Plasmid uptake was verified through colony PCR. Positive colonies were selected for plasmid isolation and sent to Eurofins for sequencing.

Table 1. Bacterial Strains

Strain/Plasmid	Genotype	Reference/Source
E. coli		
DH5α	F- Φ80*lac*ZΔM15 Δ(*lac*ZYA-*arg*F) U169 *rec*A1 *end*A1 *hsd*R17 (rk-, mk+) *pho*A *sup*E44 λ-*thi*-1 *gyr*A96 *rel*A1	Invitrogen
DH5α λ-pir	supE44, Δ*lacU169 hsd*R17, *rec*A1 *end*A1 *gyr*A96 *thi*-1 *rel*A1, λpir	(36)
SM10 λ-pir	*thi thr leu tonA lacY supE recA::RP4-2-Tc::MuλpirR6K;* Km^R	(71)
AK411	DH5α with pEV1	This study
AK415A	DH5α λ-pir with pEV2	This study
AK419	DH5α with pEV3	This study
AK420	SM10 λ-pir with pEV2	This study
AK423	DH5α with pEV3	This study
AK431	DH5α with pEV4	This study
AK511	DH5α with pEV5	This study
V. cholerae		
PW357	MO10 *lacZ::vpsLp* → *lacZ,* SM^R	(38)
AK160	PW357 Δ*potD1*	(16)
AK314A	PW357 *nspC::kan*	(16)
AK429	PW357 *ΔpotA*	This study
AK440	AK429*ΔpotA* with pEV4	This study
AK449	AK314A *ΔpotA*	This study
AK454	AK449 with pEV4	This study
AK499	AK429 with pACYC184	This study
AK501	AK449 with pACYC184	This study

Table 2. Plasmids

Plasmid	Genotype	Reference/Source
pCR2.1-TOPO	plasmid for TOPO cloning, Ap^R	Invitrogen
pWM91	*oriR*6k, *lacAα*, *sacB*, homologous recombination plasmid, Ap^R	Metcalf *et al.,* 1996
pACYC184	cloning plasmid, low copy, Tet^R	New England Biolabs
pEV1	pCR2.1:: Δ*potA*	This study
pEV2	pWM91::Δ*potA*	This study
pEV3	pCR2.1::*potA-V5*	This study
pEV4	pACYC184::*potA-V5*	This study
pEV5	pCR2.1:: Δ*potD3*	This study

Table 3. Primers

Primer	Description	Sequence
PA242	Forward primer of upstream fragment of *potA* for deletion	5'-GCGCGGATAACGTCACGC-3'
PA243	Reverse primer of upstream fragment of *potA* + SOE for deletion	5'-TTACGAGCGGCCGCAACCACAGCCCGATGGACCTAG-3'
PA244	Forward primer of downstream fragment of *potA* + SOE for deletion	5'-TGCGGCCGCTCGTAAATCGGACAGAAAGTTGCCGTC-3'
PA246	Reverse primer of downstream fragment of *potA* for deletion	5'-GGTGCGGATGAGTGAGTTGG-3'
PA251	Forward primer of *potA* for complement	5'-CCATGGCTACAGGTCCAACAAGTAGG-3'
PA252	Reverse primer of *potA* + V5 for complement	5'-CCATGGCTACGTAGAATCGAGACCGAGGAGAGGGTTAGGGATAGGCTTACCGCCGCTGCCGCTGCCAGCTTTTTGCTCATCATTGAGG-3'
PA258	Reverse primer of *potA* + V5 for complement with corrected NCOI site	5'-CCATGGCTACGTAGAATCGAGACCG-3'
PA271	Forward primer of *potA-potB* intergenic region	5'-CCGGTATGTGTGTGATGGTTAG-3'
PA272	Reverse primer of *potA-potB* intergenic region	5'-CATCAGGTTGGGGATCAGTAC-3'
PA273	Forward primer of *potB-potC* intergenic region	5'-GGTGCCGCAACCAGTATTG-3'
PA274	Reverse primer of *potB-potC* intergenic region	5'-CCGCCCCATTTGATACC-3'
PA287	Forward primer of *potC-potD2* intergenic region	5'- CTGAAGTAAACGCACTGGCG-3'
PA288	Reverse primer of *potC-potD2* intergenic region	5'- GCTCCAAACTAAACGTTGCCC-3'
PA289	Forward primer of *potD2-potD1* intergenic region	5'- CCGTTGGCGATAAGACAGTG-3'
PA290	Reverse primer of *potD2-potD1* intergenic region	5'- GCTGCGCACAGAGCACTC-3'
PA293	Forward primer of upstream fragment of *potD3* for deletion	CCCAACCGATCGCTGTAACGCC
PA294	Reverse primer of upstream fragment of *potD3* +SOE for deletion	5'-TTACGAGCGGCCGCACACGACATCGTAACCAGTGCC-3'
PA295	Forward primer of downstream fragment of *potD3* +SOE for deletion	5'-TGCGGCCGCTCGTAAGGTCGAGCGCTGCTACCG-3'
PA296	Reverse primer of downstream fragment of *potD3* for deletion	5'-CACCGAAGGTGGAGCTCATC-3'

Western Blotting

Cells were grown overnight in 3mL of LB broth at 37°C and with shaking at 200 rpm. Cells were then pelleted at 16,100 rpm for 2 minutes, resuspended in 300µL 1X PBS, sonicated on ice three times for 10-15 seconds each, and centrifuged for 2 minutes at 16,500 rpm. The supernatant was removed and diluted 1:1 with Laemlli Buffer containing 2-Mercaptoethanol, then incubated at 65°C for 15 minutes. Fifteen microliters were then loaded to a SDS-polyacrylamide gel consisting of a 12% resolving gel and a 5% stacking gel and run at 150V for 1 hour and 15 minutes. Subsequently, proteins were transferred onto a PVDF membrane by briefly immersing a PVDF membrane in methanol, then placing both gel and membrane in 1X Transfer Buffer and equilibrating for 15 minutes. Gel and membrane were then run at 100V for 1 hours in a BIO-RAD Mini Trans-Blot (Hercules, CA). The PVDF membrane was blocked overnight by immersing in a mixture of 5% skim milk and 1X PBS and incubating at 4°C with shaking. The following day, the membrane was washed with PBS with 0.05% Tween 20 (PBST), then incubated on a rotator in 10 mL of 3% skim milk/PBS with monoclonal anti-V5 antibody conjugated to horseradish peroxidase diluted 1:20,000 for one hour at room temperature. The membrane was then washed in PBS with 0.05% Tween 20 for fifteen minutes. Two more PBST washes were performed, each for 5 minutes. Once washed, the membrane was incubated with 2 mL of SuperSignal West Pico Chemiluminescent Substrate (Thermo Scientific, Rockford, IL) for 5 minutes. Imaging was performed using a BIO-RAD Molecular Imager® Gel Doc™ XR System (Hercules, CA).

Confirmation of cotranscription of pot genes

Planktonic cells were grown in a 2 mL LB culture overnight at 27°C with shaking as previously described. Cells were then diluted 1:50 in 10 mL and grown to mid-log phase (OD_{600} of 0.4.) Cells were then washed three times in 10 mL 1X PBS and suspended in Stock Buffer (2.5 mM sodium azide, 50 mM Tris base, 25 mM $MgCl_2$ at pH 7.2). Cells were pelleted, supernatant removed, and pellets were air-dried. Once dried, the pellet was flash frozen in a dry ice-EtOH bath. Frozen cells were lysed by addition of 1 mL TRIzol reagent and rapid pipetting for 30 seconds. Cells were then incubated at room temperature for 5 minutes. Following incubation, 1 mL chloroform was added and samples were mixed well. Samples were then incubated at room temperature for 3 minutes, then centrifuged at 12,000 x g for 20 minutes at 4°C in order to separate and remove the aqueous phase containing RNA. Isopropanol was added and samples were incubated at -20°C overnight in order to precipitate RNA. The following day, RNA was extracted by pelleting at 12,000 x g for 20 minutes at 4°C. RNA was then washed twice in 100% EtOH and resuspended in nuclease-free water. Following resuspension RNA was purified with Qiagen RNeasy Mini Kit (Hilden, Germany) following manufacturer's instructions. cDNA was synthesized by reverse transcribing 2.5 µg of RNA using the Superscript VILO Kit (Invitrogen, Carlsbad, CA) following manufacturer's instructions. Junction primers were generated to anneal ~100 bp upstream of the stop codon of *potA* and ~100 bp downstream of the start codon of *potB* to amplify 203 bp of the *potA-B* junction; ~100 bp upstream of the stop codon of *potB* and ~100 bp downstream of the start codon of *potC* to amplify 219 bp of the *potB-C* junction; ~40 bp upstream of the *potC* stop codon and ~130 bp downstream of the *potD2* start codon to amplify 221 bp of the *potC-potD2* junction; and ~10 bp downstream of the *potD2* stop codon and ~125 bp downstream of the *potD1* start codon to amplify 251 bp of the *potD2-potD1*

junction. PCR was performed with junction primers and OneTaq polymerase. PCR products were run on an agarose gel in order to visualize junction fragments.

Polyamine extraction, benzoylation, and HPLC analysis

Overnight cultures in 3 mL tryptone media were incubated at 27°C with shaking as previously described. Cells were diluted 1:50 into either 20 mL or 50 mL tryptone. Cultures were grown to mid log phase and pelleted at 5000 rpm for 7 minutes at room temperature. Supernatant was removed and cells were washed with 1X Phosphate Buffered Saline (PBS), and resuspended in deionized water at 10 μL/mg of wet weight. Following resuspension, cells were lysed by sonication using a Heat Systems Ultrasonics Inc (Newtown, CT). W-380 Sonicator set to 40% duty cycle and output control of 5 for 6 seconds. Lysates were centrifuged at 16,100 rpm for 10 minutes to pellet cell debris, and the supernatant containing polyamines was removed. Proteins and other macromolecules were precipitated by adding 5% trichloracetic acid and centrifuged at 16,100 rpm for one minute. Supernatant containing polyamines was removed.

Polyamines were then benzoylated to allow detection through HPLC. Cellular extracts containing polyamines were diluted 1:1 with water for a total volume of 500 μL. 2 mL of 2 M NaOH was added to each sample and mixed. Benzoyl chloride (Sigma) was diluted in HPLC grade methanol (EMD Millipore Corporation, Darmstadt, Germany) to 25%, and 20 μL of this solution was then added to each sample. Samples were mixed by vortex for one minute, then incubated at room temperature with shaking at 150 rpm for one hour. Following incubation, 1 mL chloroform was added to each sample tube, mixed well, and centrifuged at 3,320 rpm. The chloroform layer was removed, and this step was repeated. The combined chloroform fraction was then washed with 1 mL of deionized water and centrifuged at 3,320 rpm for one minute.

Chloroform layer was then removed, and chloroform was evaporated to dryness. Dry polyamines were then resuspended in 100 μL of 60% methanol, 40% water.

HPLC analysis was performed utilizing a Waters 1525 Binary Pump. Polyamines were detected with a Waters 2487 Dual Wavelength Absorbance Detector set at 254 nm. Samples were run through a Phenomenex 4.0 x 30 mm guard cartridge and Spherclone 5micro ODS column. For each sample, 40 μL was injected and run through the column using a gradient of 45-60% methanol in water for 45 minutes, with a 10 minute isocratic equilibration of 45% methanol in water.

Biofilm assay

An isolated colony was used to inoculate a 2 mL tryptone culture, and incubated overnight at 27°C with shaking at 200 rpm. This culture was diluted 1:50 in 2 mL the following morning, grown to an OD_{595} of 0.3-0.4, then normalized to an OD_{595} of 0.04 in 300 μL of tryptone media. Cultures were incubated at 27°C for 24 hours without shaking. Following incubation, 150 μL of planktonic cells was removed with a micropipette added to a microtiter plate. The remaining planktonic cells were discarded. The biofilm was washed with PBS and dispersed by vortexing with glass beads. Using a micropipette, 150 μL of dispersed biofilm was added to a microtiter plate, and cell densities were measured at OD_{595} using a BIO-RAD Microplate Reader model 680.

Zebrafish infection

Bacterial cultures were grown overnight for 16-18 hours at 27°C with shaking at 200. A Δ*potA* mutant strain carrying a *vpsLp-lacZ* fusion allowed differentiation between mutant and

wild-type strains by plating on LB with X-gal, because wildtype *V. cholerae* lacks *β*-galactosidase activity. Following overnight incubation, cultures were diluted 1:20 and grown to an O.D. of 0.4. Cultures were then washed three times in PBS to remove antibiotics, and 100μL of the washed cultures was resuspended in 1 mL of PBS, and then added to the respective tanks. At this time, 1 mL water samples were taken from each tank to determine the total number of bacterial cells in the initial inoculum. For each strain tested, a control tank containing no fish was also inoculated. Experimental tanks contained four fish in 500 mL of water. In addition, a control tank containing four fish in 500 mL of water was set up with no bacterial cultures added. Fish were incubated with the added *V. cholerae* for approximately 20 hours, after which they were sacrificed by addition of Tricaine to the tank water at a concentration of 300 mg/L. Water samples were taken at the time of euthanasia to determine bacterial load of tank water.

Following euthanasia, fish were rinsed in 70% EtOH and blotted dry. Intestines were aseptically removed using a dissecting microscope and homogenized in sterile PBS solution. Using sterile PBS solution, 3 serial dilutions were performed on each fish and water sample taken. These dilutions were plated on LB agar containing streptomycin at 100 μg/mL, to which the strains of *V. cholerae* used for infection are resistant. Plates were incubated overnight at 27°C as previously described to allow for significant bacterial growth, after which colonies were patched on thiosulfate-citrate-bile salts-sucrose (TCBS) agar in order to differentiate *V. cholerae* from background growth of endogenous fish intestinal bacteria also resistant to streptomycin. Colonies were then plated on LB with 100 μg/mL streptomycin and 40 μM X-gal in order to determine wildtype and Δ*potA* colony forming units (CFUs) using a blue-white screen. Following these counts, CFUs were calculated based on the known dilution factors, and colony-forming unit counts of mutants were compared to wildtype in order to determine the proficiency

of the mutants to colonize. Experiments were performed in accordance with IACUC protocol #12-10.

Results

Construction of a V. cholerae ΔpotA mutant

In order to characterize the role of the PotA protein in polyamine uptake through the PotABCD1 ABC-type transport system, I first constructed a deletion in the *potA* gene. A region of approximately 400 base pairs upstream of the *potA* gene was amplified using primers PA242 and PA243, shown in Figure 11 lanes 2 and 3. PA242 and PA243 were designed to anneal to the regions 301 bp upstream from the start codon of *potA* and 144 bp downstream from the start codon of *potA,* respectively. Separately, a region downstream of the *potA* gene of approximately 400 bp was amplified using primers PA244 and PA246, designed to anneal 71 bp upstream from the stop codon, and 234 bp downstream from the stop codon, respectively. The downstream region is shown in Figure 11, lanes 4 and 5.

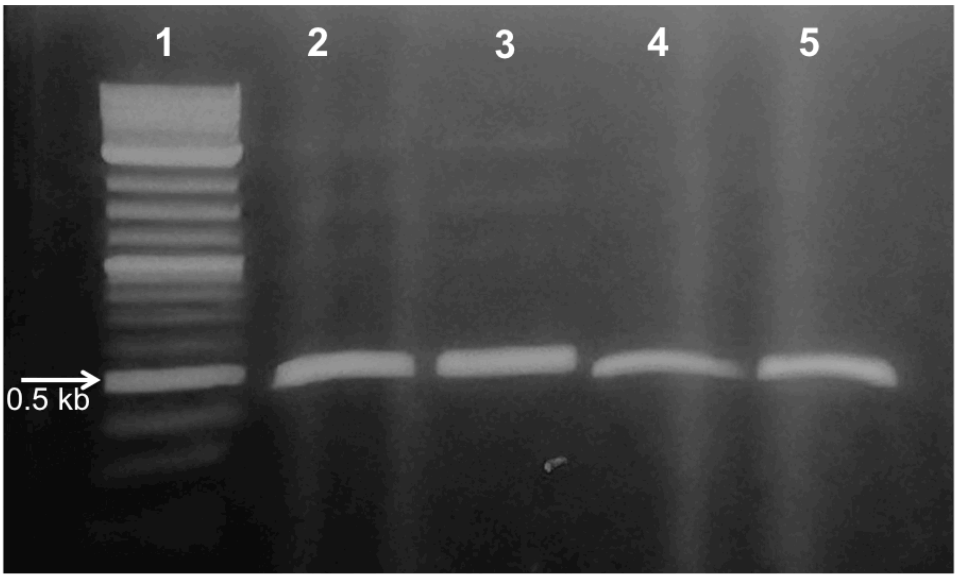

Figure 11. Gel electrophoresis of pEV2 fragment amplification. This image depicts the two fragments constructed to generate an in-frame deletion in the *potA* gene. Lane 1 is 2-log ladder, lanes 2 and 3 are the 445 bp upstream fragment, lanes 4 and 5 are the 386 bp downstream fragment.

PA243 and PA244 were constructed with complimentary overhangs to each other in order to facilitate removal of 918 bp of the total 1,133 bp of the *potA gene*. The upstream and

downstream fragments were added to a reaction together with PA242 and PA246, denatured, and re-annealed in order to allow this splicing by overlap extension (SOE) deletion to take place. Generation of this recombinant molecule at 831 bp was verified by gel electrophoresis as shown in lane 3 in Figure 12.

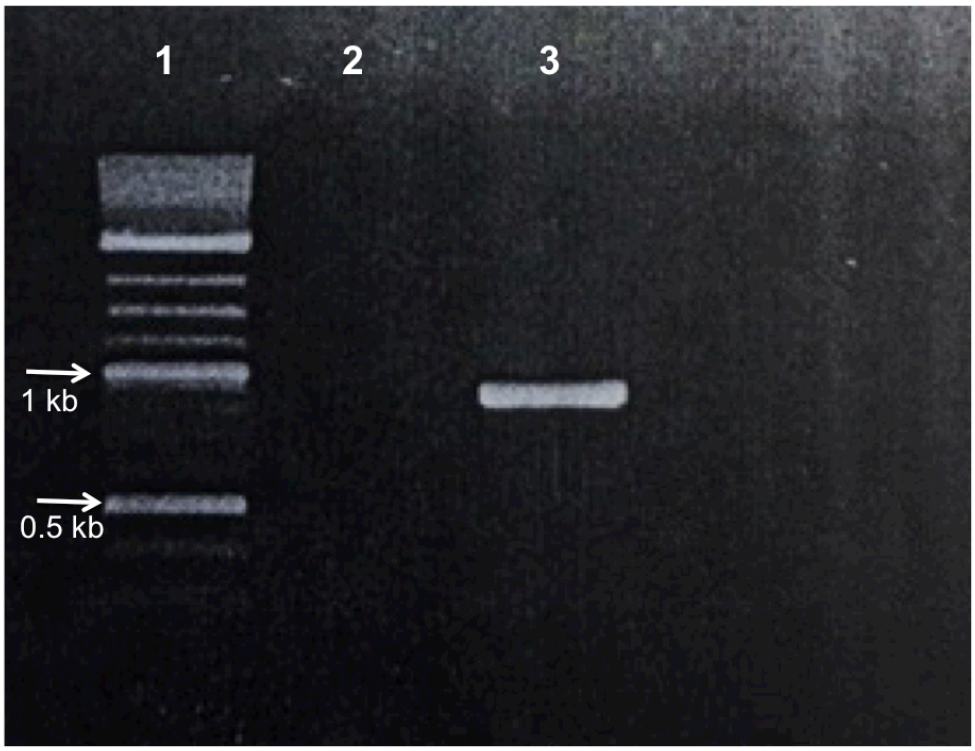

Figure 12. Gel electrophoresis of the pEV2 fused product. This image depicts the fused upstream and downstream fragments at 831 bp in length. Lane 1 contains the 2-log ladder, lane 3 contains the fused Δ*potA* product.

This fragment was purified, adenylated at the 3' ends, and cloned into pCR2.1 TOPO plasmid. This constructed plasmid was then electroporated into *E. coli* DH5α. A colony PCR was performed in order to verify uptake of the pEV1 plasmid, shown in Figure 13 lanes 3-7.

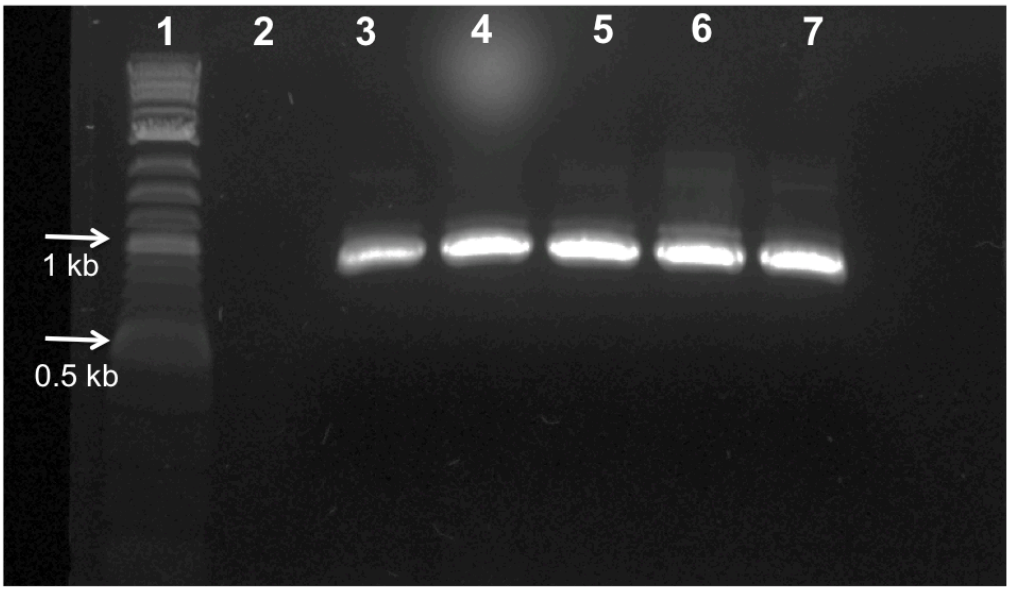

Figure 13. Colony PCR of *E. coli* DH5α transformed with pEV1. Lane 1 contains the 2-log ladder, lanes 3-7 contain fragments from colonies positive for the insert.

Two of these colonies were selected for plasmid extraction and the plasmids were sequenced for verification. The Δ*potA* fragment was digested out of pCR2.1 using XhoI and SpeI enzymes, and ligated into pWM91 linearized with the same enzymes. This pEV2 plasmid was electroporated into *E. coli* DH5α-λpir. Uptake of pEV2 was verified by colony PCR, shown in Figure 14.

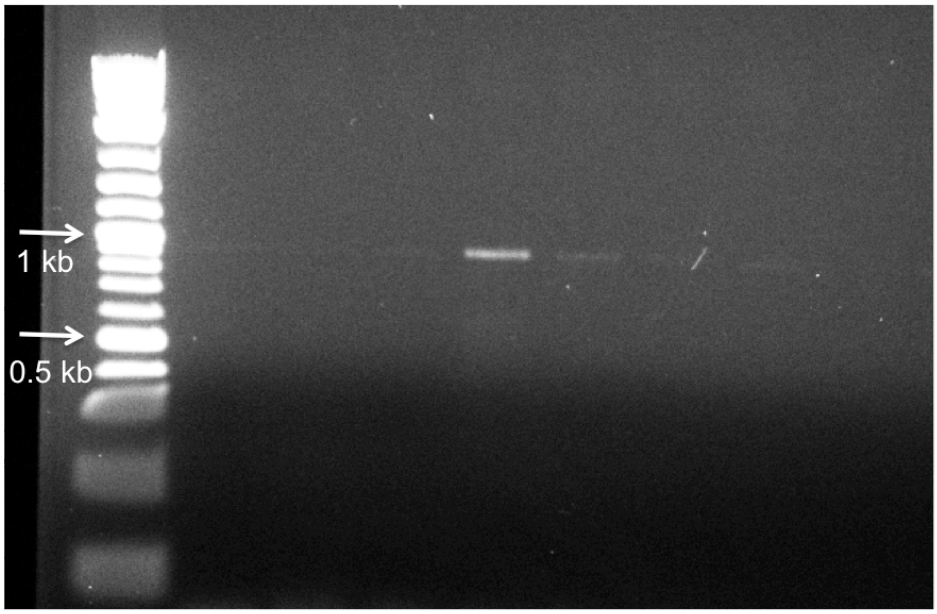

Figure 14. Colony PCR of *E. coli* DH5α-λpir transformed with pEV2. Lane 1 contains the 2-log ladder, lanes 2-8 contain fragments from colonies positive for the insert.

pEV2 was then electroporated into *E. coli* SM10-λpir. Colony PCR and gel electrophoresis to were used to verify a fragment at approximately 800 bp to generate strain AK420. Positive colonies are shown in Figure 15, lanes 4-10.

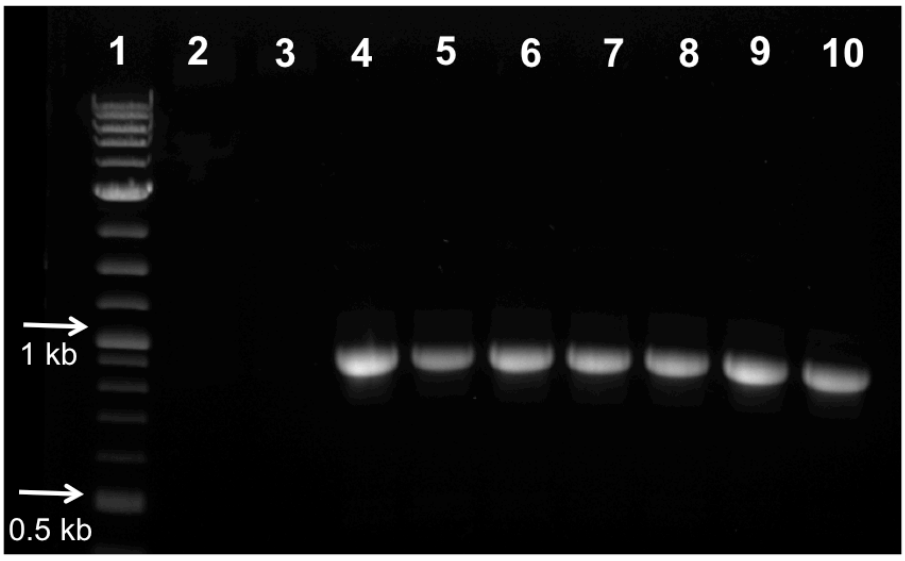

Figure 15. Colony PCR of *E. coli* SM10-λpir transformed with pEV3. Lane 1 contains the 2-log ladder, lanes 4-10 contain fragments from colonies positive for the insert.

AK420 was used for conjugation with *V. cholerae* PW357 through SacB counter-selectable mutagenesis, resulting in recombination of the Δ*potA* construct onto the *V. cholerae*

chromosome. Streptomycin resistant but ampicillin sensitive colonies were screened for Δ*potA* integration through colony PCR and gel electrophoresis. Amplification of DNA from one colony positive for plasmid uptake is shown in Figure 16, lane 20. The approximately 1700 bp fragment in fragments 2-19 represents the full-length *potA* gene with 535 bp of the flanking regions on either side.

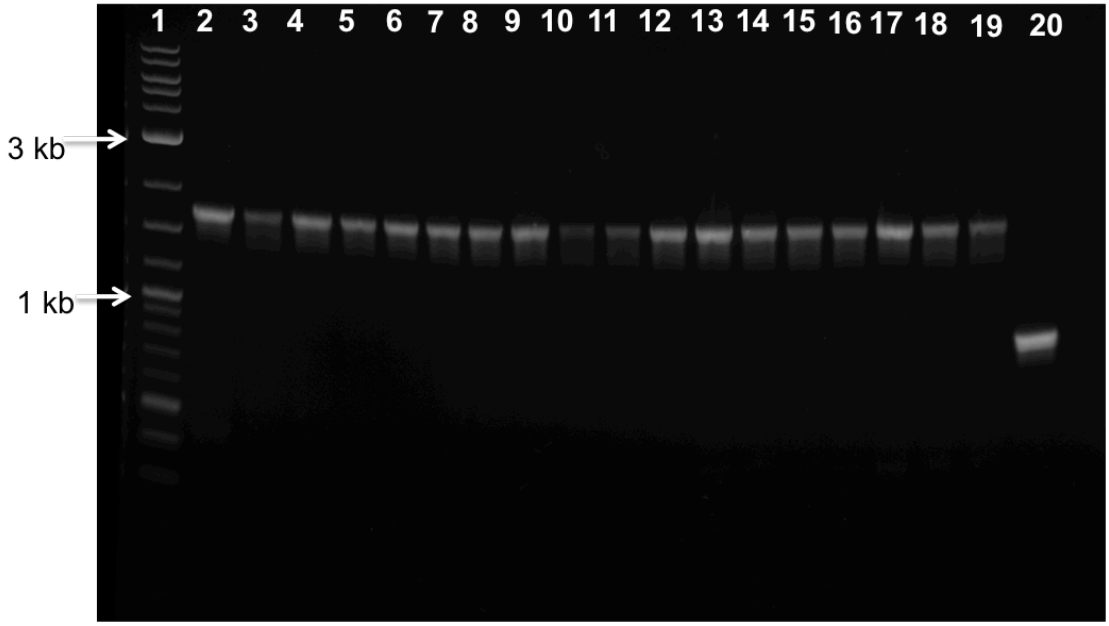

Figure 16. Colony PCR to confirm *potA* deletion in *V. cholerae* PW357 background. Lane 1 contains 2-log ladder. Lanes 2-19 contain PCR product from colonies that contained the full-length *potA* gene. Lane 20 contains PCR product from a colony in which recombination resulted in a chromosomal incorporation of the Δ*potA* constructed fragment.

Construction of a nspC::kan ΔpotA double mutant

Because *V. cholerae* is capable of synthesizing norspermidine *de novo,* construction of a double mutant was necessary in order to quantify intracellular norspermidine as a measure of only uptake. This was generated by using strain AK314A (*V. cholerae* PW357 *nspC::kan*) as the recipient strain in the same SacB counter-selectable mutagenesis procedure with the donor strain AK420 carrying pEV2. Kanamycin and streptomycin resistant but ampicillin sensitive colonies

were screened for deletion of the *potA* gene through colony PCR and gel electrophoresis, shown in Figure 17, lanes 5, 7, 8, 10, and 12.

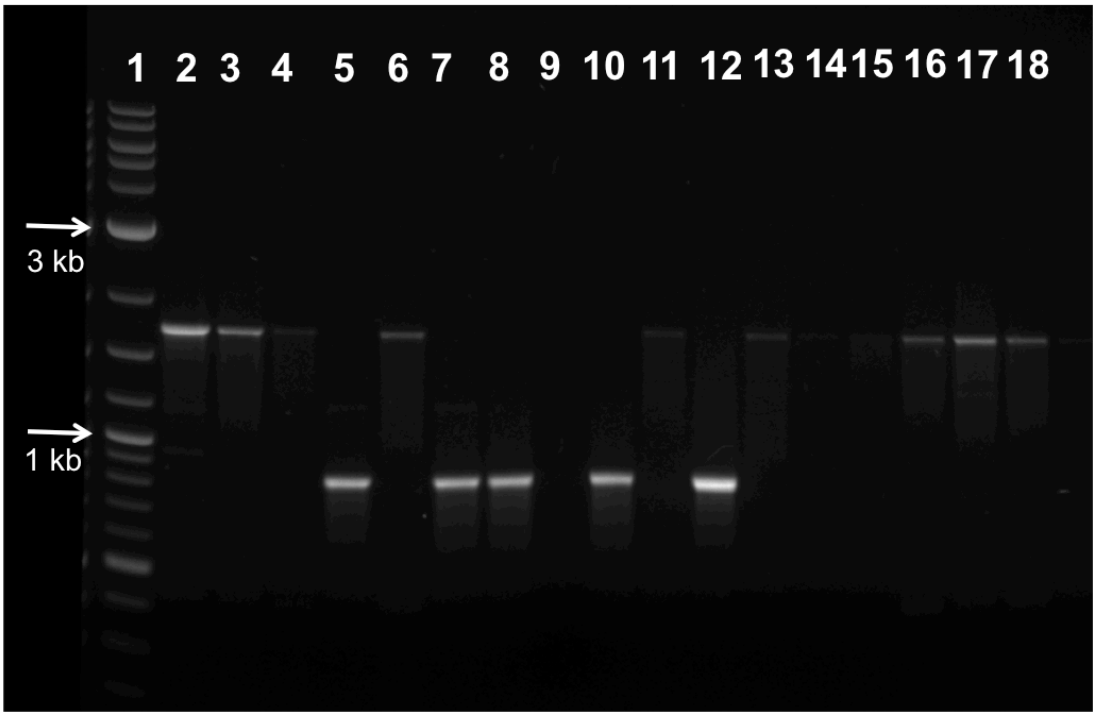

Figure 17. Colony PCR to confirm *potA* deletion in *nspC::kan* background. Lane 1 contains 2-log ladder. Lanes 2-4, 6, 11, 13, and 16-18 contain PCR product from colonies with intact *potA*. Lanes 5, 7,8,10, and 12 contain PCR product from colonies in which recombination resulted in incorporation of the Δ*potA* construct into the *V. cholerae* chromosome. Lanes 9, 14 and 15 contained PCR products that failed to amplify.

Complementation of ΔpotA strains with potA-V5

In order to verify the role of PotA in uptake of norspermidine and spermidine, the Δ*potA* mutant was completmented with a plasmid containing the *potA* gene. Primers were constructed to amplify the full *potA* gene, as well as add a V5 tag for detection via western blot. This fragment was generated by amplifying chromosomal *V. cholerae* MO10 DNA with primers PA252 and PA258. Generation of a product at 1,240 bp was verified by colony PCR and gel electrophoresis, shown in Figure 18 Lane 3.

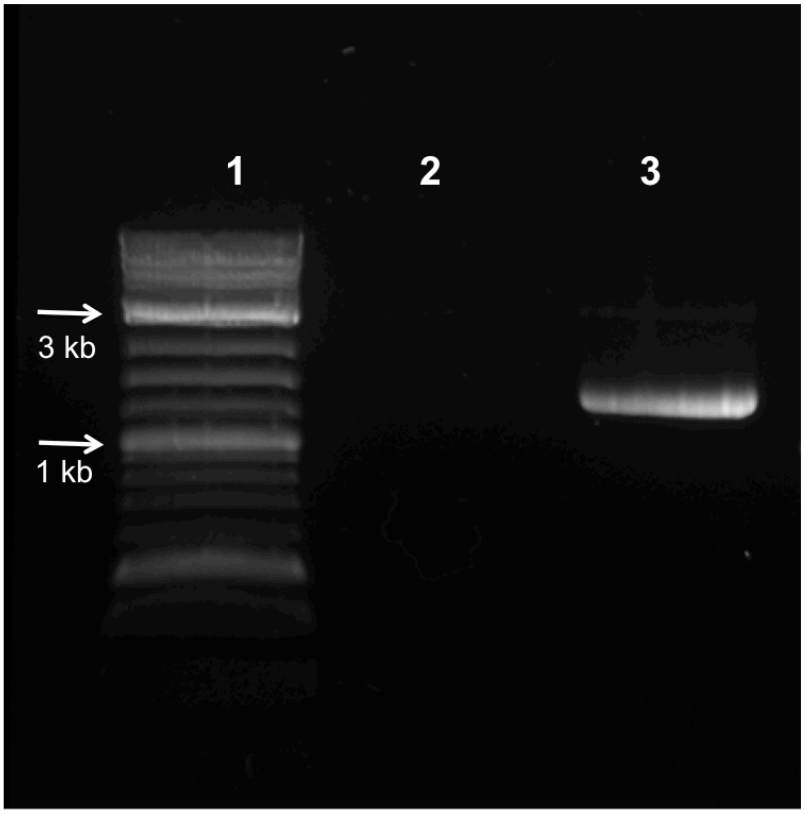

Figure 18. Gel electrophoresis of pEV4 fragment construction. This image depicts the amplification of the *potA-V5* fusion product. Lane 1 contains the 2-log ladder, lane3 contains the 1,240 bp fusion product.

The fragment was purified, adenylated at the 3' ends, and cloned into pCR2.1 TOPO plasmid. The pEV3 plasmid was then electroporated into *E. coli* DH5α. Uptake of the plasmid was checked through colony PCR and gel electrophoresis. Positive colonies are shown in Figure 19, lanes 4, 6, 8 and 9.

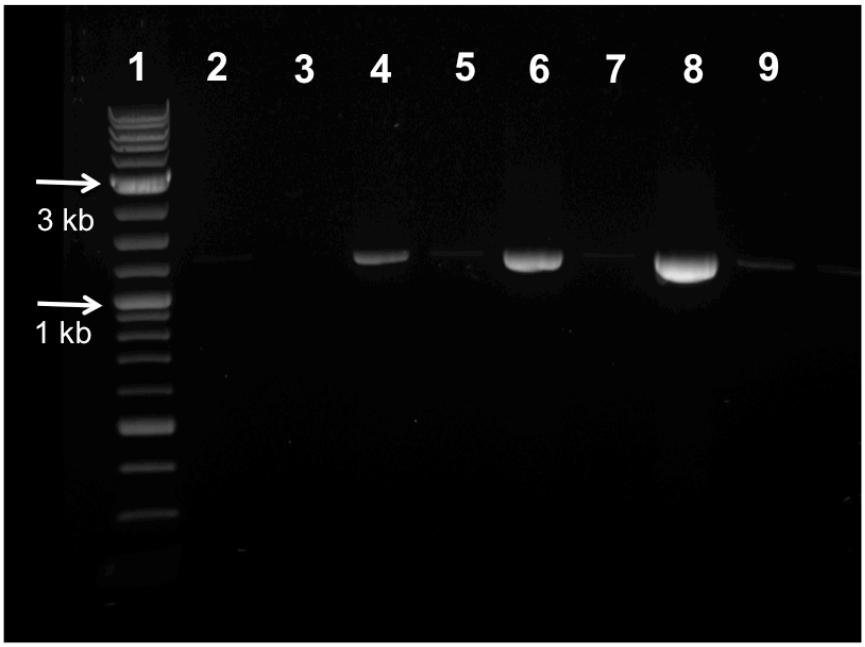

Figure 19. Colony PCR of pEV3 in *E. coli* DH5α. Lane 1 contains 2-log ladder, lane 4 contains a colony positive for pEV3 amplification, lane 5 contains PCR product from a colony that failed to amplify or lacks the insert, lane 6 contains PCR product from a colony positive for the insert, lane 7 contains PCR product from a colony that failed to amplify or lacks the insert, lanes 8 and 9 contain PCR product from colonies positive for the insert.

Positive colonies were selected for plasmid isolation and purification. Plasmids were then sent to Eurofins for sequence verification. Following sequencing, the fragment was removed from pCR2.1 by digesting with NcoI and ligated into pACYC184 linearized with the same enzyme and dephosphorylated with calf intestinal alkaline phosphatase on the 5' ends in order to prevent recircularization of the plasmid during ligation. pEV4 was then electroporated into *E. coli* DH5α and verified by colony PCR, shown in Figure 20 lanes 2-8.

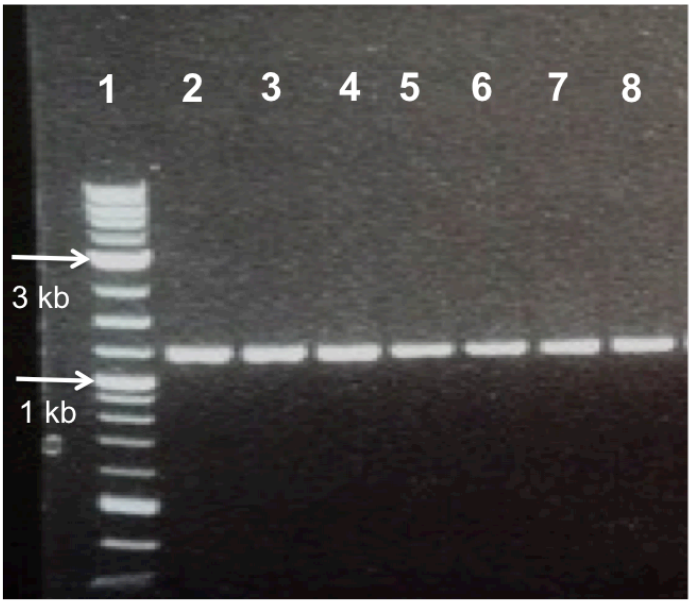

Figure 20. Colony PCR of pEV4 in *E. coli* DH5α. Lane 1 contains 2-log ladder, lanes 2-8 contain PCR product from colonies positive for *potA-V5* insert.

A positive colony was selected for pEV4 plasmid isolation. pEV4 was then electroporated into *V. cholerae* AK429 (Δ*potA*) and AK449 (*nspC::kan* Δ*potA*) to generate complemented strains. Plasmid uptake in both the single and double mutant was verified by colony PCR. Figure 21 depicts two Δ*potA* colonies positive for pEV4 uptake in lanes 3 and 4.

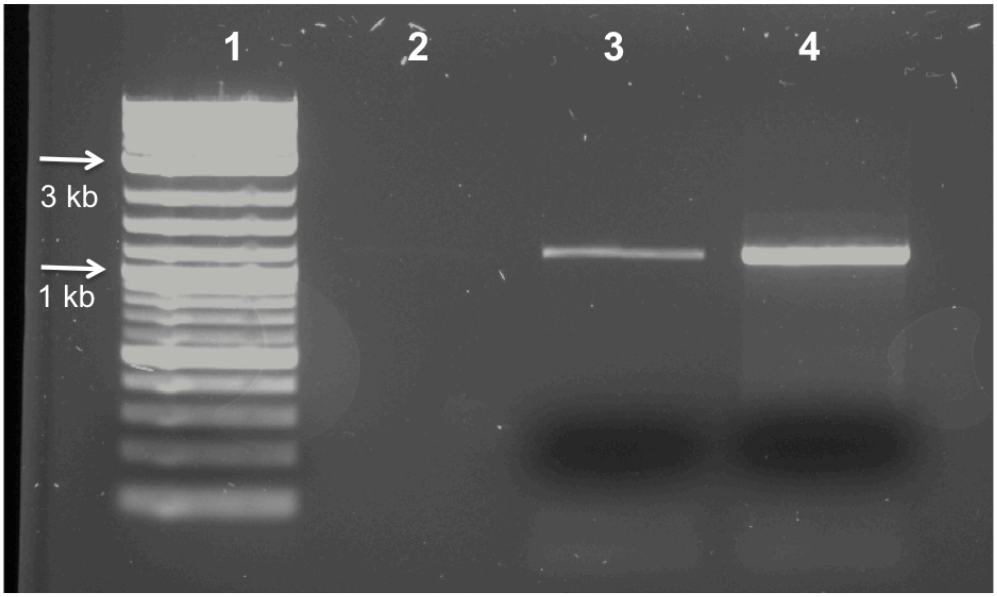

Figure 21. Colony PCR of AK429 transformed with pEV4. Lane 1 contains 2-log ladder. Lanes 3 and 4 contain PCR product from AK429 colonies positive for the pEV5 insert.

Figure 22 depicts double mutant *nspC::kan* Δ*potA* colonies positive for uptake of pEV4 in lanes 2-10.

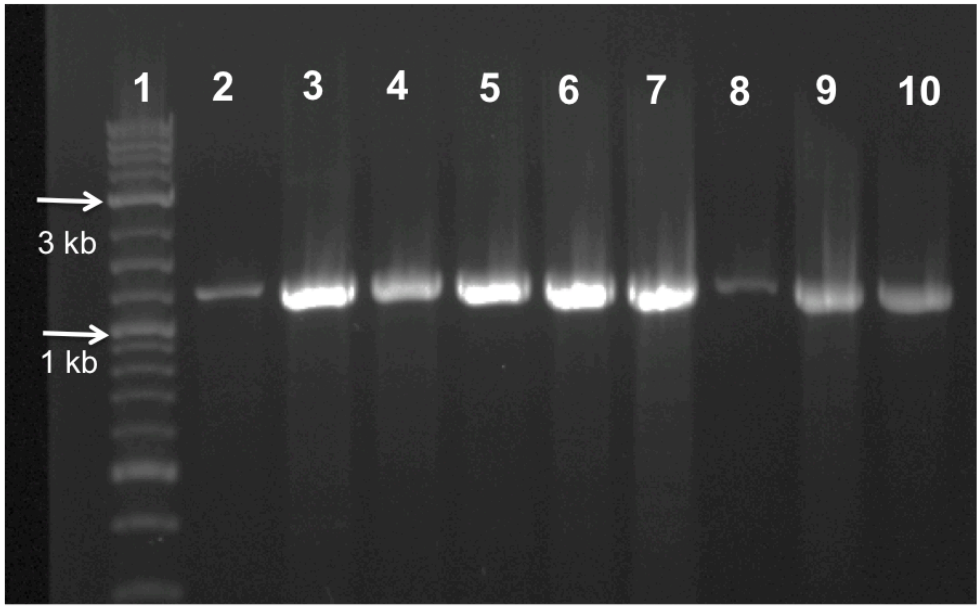

Figure 22. Colony PCR of AK449 transformed with pEV4. Lane 1 contains 2-log ladder. Lanes 2-10 contain PCR product from colonies positive for pEV5 insert amplification.

Confirmation of PotA expression

A Western blot was performed to confirm that complementation with pEV4 carrying *potA-V5* was successful, and that PotA was being expressed under the experimental conditions used. Following extraction from *nspC::kan ΔpotA* with pACYC184::*potA-V5*, proteins were separated through SDS-PAGE gel electrophoresis and transferred onto a PVDF membrane. Proteins were detected with an antibody to the V5 epitope linked to horseradish peroxidase, and visualized using horseradish peroxidase chemiluminescent substrate. As shown in Figure 4, the V5-tagged PotA protein has a molecular weight of about 47 kDa, and is present in lanes 1, 2, and 3.

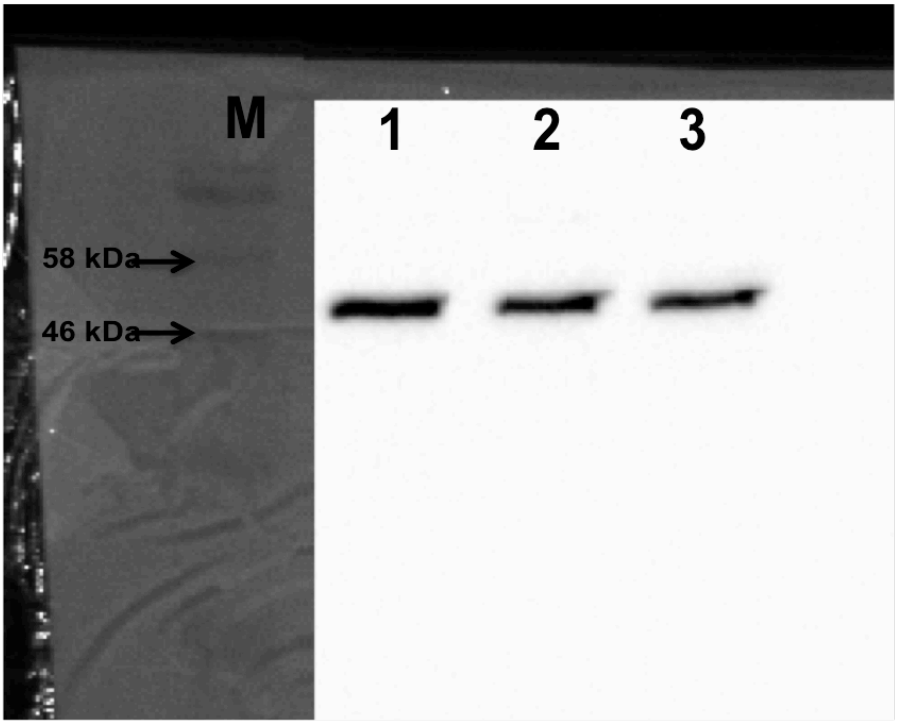

Figure 23. Confirmation of successful complementation of *nspC::kan ΔpotA* with pACYC184::*potA-V5*. In triplicate, cell lysates were separated by SDS-PAGE, transferred onto a PVDF membrane, and reacted with a V5 antibody. "M" denotes the protein marker, while lanes 1, 2, and 3 each contain extract from one biological replicate of *nspC::kan*^{R} *ΔpotA* with pACYC184::*potA-V5.* PotA-V5 is predicted to be approximately 47 kDa.

PotA is required for import of norspermidine

Because PotB, PotC, and PotD1 have demonstrated a role in norspermidine import, the role of PotA in norspermidine uptake was analyzed in order to determine that each component of the system is essential to facilitate import, and to further characterize this novel norspermidine importer. *V. cholerae* is capable of synthesizing norspermidine from diaminopropane through the enzymes CANSDH and CANSDC. The latter is encoded by *nspC*. In order to quantify norspermidine acquisition solely through uptake, strain AK449 was used for norspermidine uptake analysis. This strain contains a kanamycin acetyltransferase cassette disruption of the *nspC* gene, functionally preventing norspermidine synthesis, and thus allowing quantification of intracellular norspermidine acquired only through uptake. As shown in Figure 24 panel B, the

nspC::kan control strain contains putrescine, diaminopropane, cadaverine, and norspermidine when media is supplemented with 100 μM norspermidine. This strain contains no norspermidine when grown in the absence of added norspermidine. Although norspermidine synthesis has been disrupted in this strain, it may still be acquired through import by the PotABCD1 system. The abundance of exogenous norspermidine also prevents spermidine import, most likely by outcompeting spermidine for binding sites. As shown in Figure 24 panel C, the *nspC::kan* Δ*potA* mutant, shown in gray, contained no intracellular norspermidine when culture media was supplemented with 100 μM norspermidine, demonstrating impaired uptake of norspermidine. When complemented with pEV4, strains regained the ability to import norspermidine, demonstrating that PotA has an essential role in uptake of norspermidine uptake through PotABCD1.

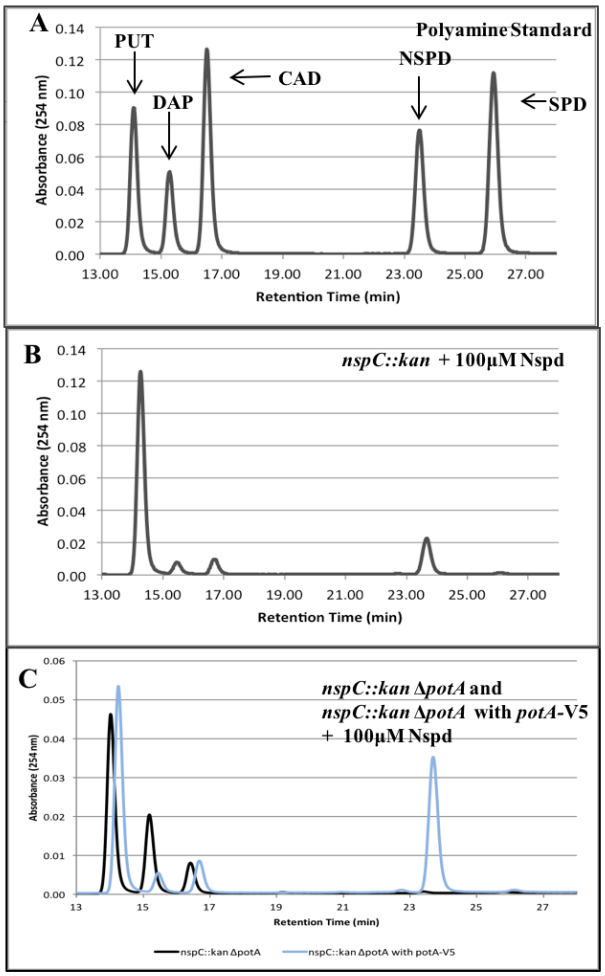

Figure 24. PotA is required for norspermidine import. HPLC chromatograms of extracted and benzoylated cellular polyamines. Only retention times between 13 and 28 minutes are shown. (A) Polyamine standard including putrescine (PUT), diaminopropane (DAP), cadaverine (CAD), norspermidine (NSPD), and spermidine (SPD). (B) Chromatogram of polyamines extracted from *nspC::kan,* AK314A. (C) Chromatogram of polyamines extracted from *nspC::kan* Δ*potA,* AK449, in black overlayed with chromatogram of polyamines extracted from *nspC::kan* Δ*potA*-V5, AK454, in gray. Norspermidine was supplied exogenously at 100 µM to (B) and (C) cultures as described in Materials and methods.

PotA is involved in import of spermidine

Because previous work in our lab has demonstrated a role for PotB, PotC and PotD1in spermidine uptake as well as norspermidine, I sought to determine whether the PotA protein is involved in this import as well. As shown in Figure 25 panel C, deletion of the *potA* gene resulted in a substantial reduction in intracellular spermidine compared to wildtype, indicating deficient spermidine uptake due to the disruption of PotA. However, a small peak did still appear at about 26 minutes retention time. This peak could result from two sources: a low

affinity spermidine transporter may import spermidine when it is available at high concentrations outside of the cell, or another molecule extracted from the cell may interact with the HPLC column in a similar manner to spermidine, leading to indistinguishable retention times. To further confirm the role of *potA* in spermidine uptake, AK429 was complemented with pEV4, containing the full *potA* gene in order to restore gene function. As shown in Figure 25, panel C, the *potA* deletion strain complemented with a plasmid carrying *potA* was capable of importing spermidine to much higher levels than the mutant strain. Restoration of spermidine import in the presence of *potA* on a plasmid provides further supporting evidence that PotA is an essential component of the PotABCD1 system, and is involved in spermidine import through this ABC-type transport system.

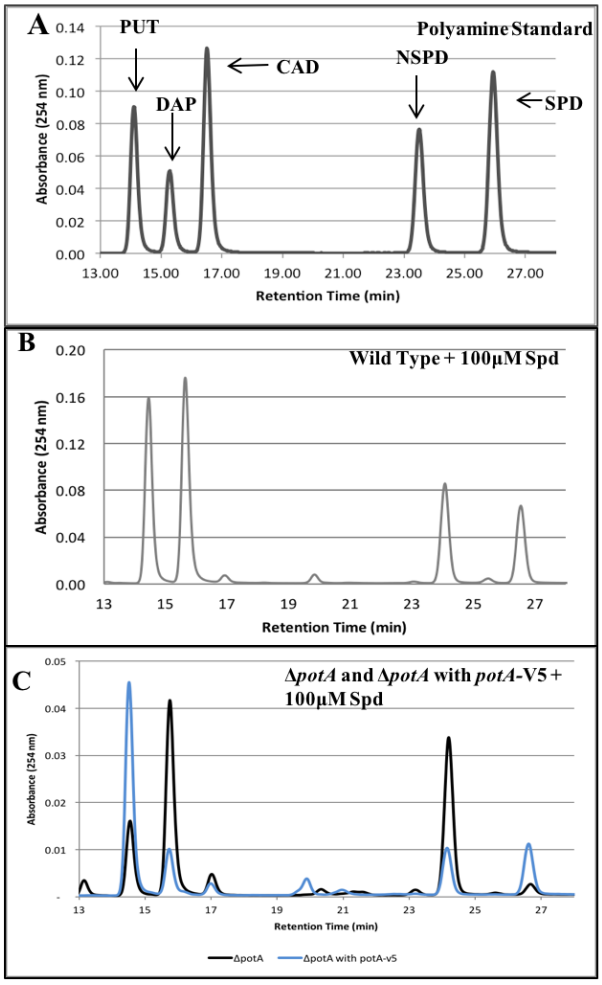

Figure 25. PotA is involved in spermidine import. HPLC chromatograms of extracted and benzoylated cellular polyamines. Only retention times between 13 and 28 minutes are shown. (A) Polyamine standard including putrescine (PUT), diaminopropane (DAP), cadaverine (CAD), norspermidine (NSPD), and spermidine (SPD). (B) Chromatogram of polyamines extracted from wildtype, PW357. (C) Chromatogram of polyamines extracted from Δ*potA*, AK429, in black overlayed with chromatogram of polyamines extracted from Δ*potA* complemented with *potA*-V5, AK440, in gray. Spermidine was supplied exogenously at 100 µM to (B) and (C) cultures as described in Materials and methods.

PotABCD1 is norspermidine-preferential

In order to determine the uptake preference of PotABCD1 for norspermidine or spermidine, polyamines were added to cultures at varying concentrations. A *nspC::kan* Δ*nspS* double mutant was used in order to allow quantification of intracellular norspermidine as only a measure of uptake, as well as removing any preferential binding of norspermidine or spermidine by NspS, which could disrupt the pool of free polyamines within the culture. Polyamines were added to cultures at concentrations of 10:1 (100 µM: 10 µM), 4:1 (100 µM: 25 µM), 2:1 (100

μM: 50 μM) and 1:1 (100 μM:100 μM). As shown in Figure 26, PotABCD1 demonstrates a strong preference for norspermidine over spermidine, and significant uptake of spermidine was not observed until it was added in 10-fold excess of norspermidine. Even in the presence of excess levels of exogenous spermidine, more norspermidine than spermidine was imported, indicating a strong preference for norspermidine over spermidine.

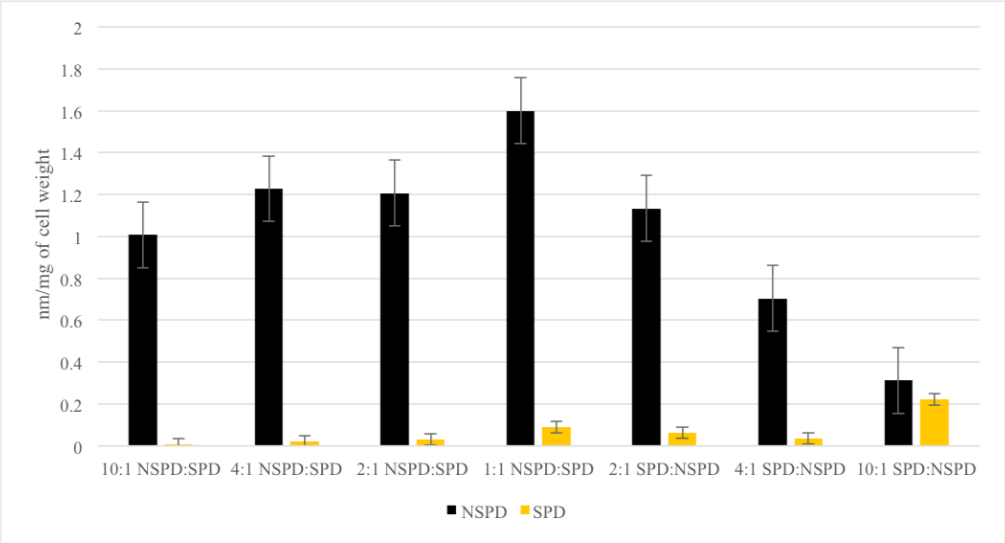

Figure 26. Uptake of polyamines through PotABCD1 is norspermidine-preferential. Norspermidine and spermidine were added to *V. cholerae nspC::kan ΔnspS* cultures at varying concentrations. The amount of polyamines in nanomoles/milligrams of cell weight were calculated by taking the are under the curve and comparing to the 40 μM polyamine standard. Error bars indicate standard deviation of three replicates.

Confirmation of cotranscription of potABCD2D1 genes

Bacterial genes that are involved in a common function are often arranged under the control of a single promoter. This organization is known as an operon. In order to fully characterize *potABCD2D1,* I sought to determine if these genes are cotranscribed. *V. cholerae* RNA was extracted and reverse-transcribed to generate cDNA. This was amplified with primers generated to amplify intergenic regions between the *pot* genes. Presence of these intergenic regions indicates cotranscription, as a single promoter will drive transcription of the entire operon. As shown in Figure 27, gene junction fragments were present between *potA* and *potB,*

potB and *potC, potC* and *potD2,* and *potD2* and *potD1*, indicating that these genes are organized in an operon and cotranscribed from a single promoter.

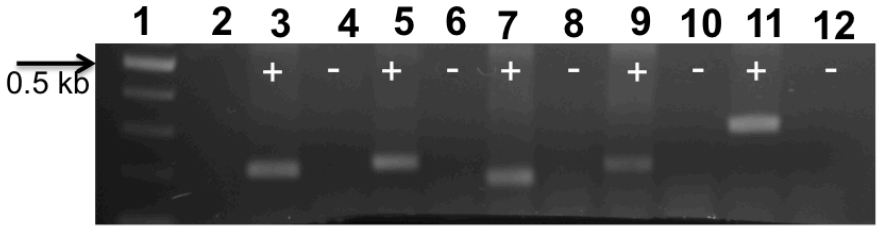

Figure 27. The *pot* genes exist in an operon, and are cotranscribed. Gene junctions between *potA/potB, potB/potC, potC/potD2, potD2/potD1*, and *vpsL/vpsM* (control) were amplified from cDNA reverse-transcribed from *V. cholerae* RNA. Lane 1 contains 2-log ladder. Lanes 3-12 contain PCR products of cDNA amplified with the following primers; lanes 3 and 4, with PA271 and PA272 to a 204 bp *potA/potB* intergenic region; lanes 5 and 6 with PA273, PA274 to a 220 bp *potB/potC* intergenic region; lanes 7 and 8 with PA287 and PA288 to a 187 bp *potC/potD2* intergenic region; lanes 9 and 10 with PA289 and PA290 to a 211 bp *potD2/potD1* intergenic region; lanes 11 and 12 with PA108 and PA109 to a *vpsL/vpsM* intergenic region. +/- indicates the presence or absence, respectively, of reverse transcriptase enzyme in cDNA reaction.

Identification of a low-affinity spermidine transporter in V. cholerae

Previous research in our lab has revealed that the Δ*potD1* mutant is capable of importing spermidine relatively high (1 mM) concentrations (20). I observed that the Δ*potD1* mutant is capable of importing spermidine at even 100 μM concentration (data not shown). This uptake appears to be dependent on the other components of the transport system, PotA, PotB, and PotC, because deletions in the transmembrane or cytoplasmic components inhibits the high level of uptake. This supports the previous hypothesis of a low-affinity transporter in *V. cholerae* that is capable of interacting with the PotABC transmembrane and cytoplasmic components in order to facilitate spermidine uptake in the absence of PotD1. We have identified *VCA1113* as a potential low-affinity spermidine transporter with 43% identity to PotD1, and refer to this gene as *potD3* (20).

Construction of a ΔpotD3 mutant

In order to determine the ability of *potD3* to act as a low-affinity spermidine transporter, I constructed an in-frame deletion in the *potD3* gene. Upstream primer PA293 was designed to anneal 179 bp upstream of the *potD3* start codon, and PA294 was designed to anneal 207 bp downstream from the *potD3* start codon. Likewise, a downstream primer pair, PA295 and PA296, was constructed to anneal to the downstream region of *potD3*. PA295 was designed to anneal 149 bp upstream from the *potD3* start codon, and PA296 were designed to anneal 193 bp downstream of the *potD3* stop codon. PCR products of approximately 400 bp were verified by gel electrophoresis and are shown in Figure 28. Fragments from the PA293-PA294 reaction are shown in lanes 3 and 4, and fragments from PA295-PA296 are in lanes 5 and 6.

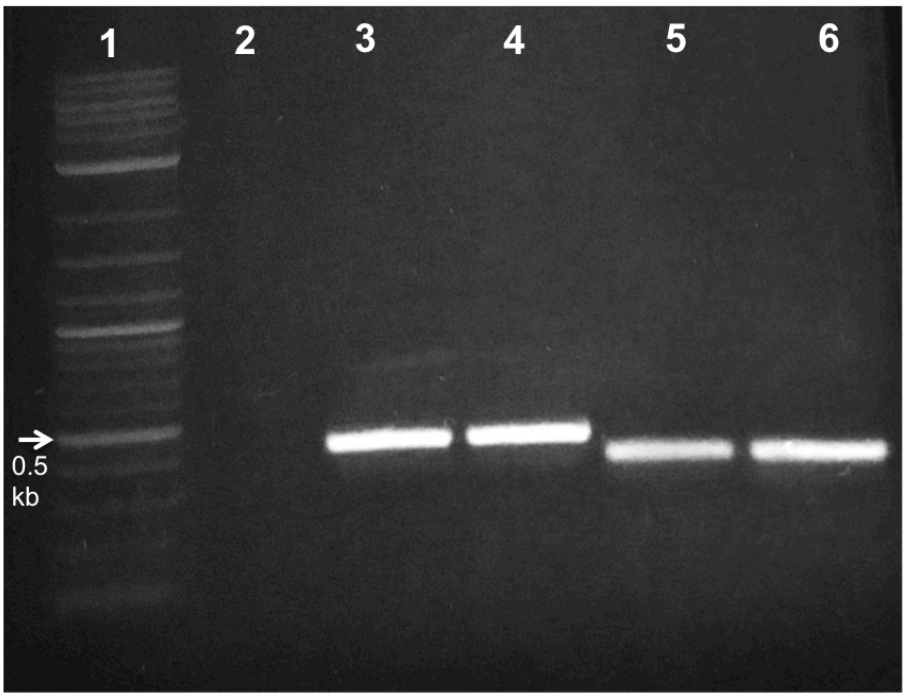

Figure 28. Gel electrophoresis of pEV5 fragment amplification. This image depicts 2 fragments constructed to generate an in-frame deletion in the *potD3* gene. Lane 1 contains 2-log ladder, lanes 3 and 4 contain the 386 bp upstream fragment, lanes 5 and 6 contain the 342 bp downstream fragment.

Fragments were combined in one PCR reaction to allow re-annealing of complementary regions on PA294 and PA295 following denaturing and resulting in an in-frame deletion of 675 bp of the total 1,031 bp gene. External primers PA293 and PA296 were added to the reaction in order to further amplify the fragment. Following PCR, fragment size was verified using gel electrophoresis, shown in Figure 29 lane 2, and PCR product was purified.

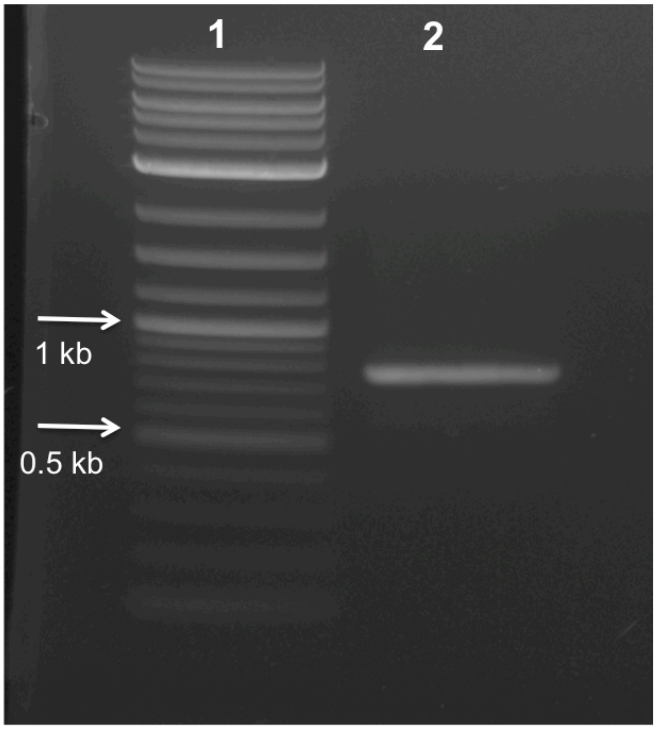

Figure 29. Gel electrophoresis of pEV5 fused product. This image depicts the fused upstream and downstream fragments at 778 bp. Lane 1 contains 2-log ladder, lane 2 contains the fused Δ*potD3* product.

This purified fragment was then adenylated at the 3' ends, and cloned into pCR2.1 TOPO plasmid. This pEV5 plasmid was then electroporated into *E. coli* DH5α. A colony PCR was performed in order to verify uptake of the pEV5 plasmid, shown in Figure 30 lanes 3 and 4. Positive colonies were selected for miniprep, and plasmids were sent to Eurofins for sequence verification. Work is ongoing in order to construct the *V. cholerae* Δ*potD3* mutant strain.

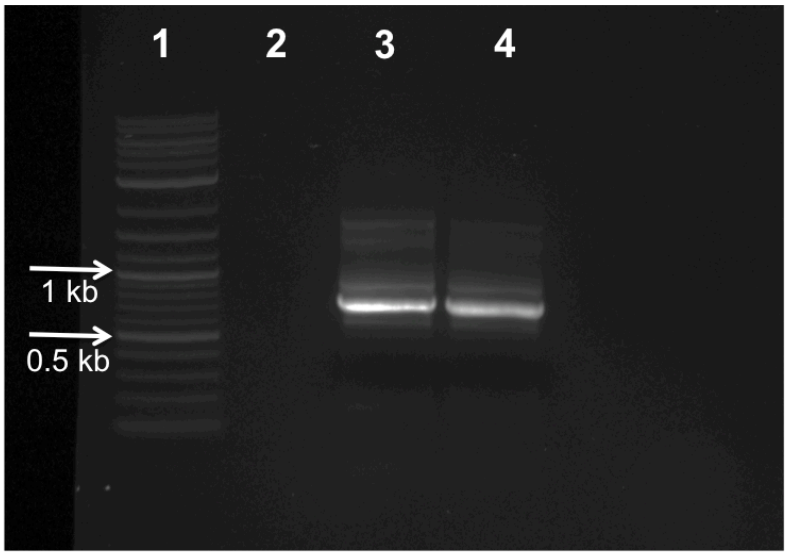

Figure 30. Colony PCR of *E. coli* DH5α transformed with pEV5. Lane 1 contains the 2-log ladder, lanes 3 and 4 contain fragments from colonies positive for the insert.

PotA is involved in biofilm formation

Previous work in our lab has shown that Δ*potB,* Δ*potC,* or Δ*potD1* mutant strains exhibit significantly higher biofilm formation compared to wildtype, supporting the role of the functional polyamine importer in modulation of the biofilm phenotype. In order to confirm the necessity of each component for transporter function, biofilm formation in the Δ*potA* strain was also analyzed. As previously observed, Δ*potB*, Δ*potC*, and Δ*potD1* strains all exhibited significantly increased biofilm formation (68, 96). Likewise, Δ*potA* strains exhibit increased biofilm formation compared to wildtype, as shown in Figure 31. A reduction in planktonic cells was also observed in all mutant strains, as is characteristic of strains that form a high amount of biofilm. Because spermidine is present in the tryptone media used for biofilm cultures at about 3-4 μM, these results indicate that polyamine transport, specifically uptake of spermidine, by the

ABC-type transporter PotABCD1 is responsible for mediation of the biofilm phenotype, rather than one of the components more directly regulating biofilm formation (16).

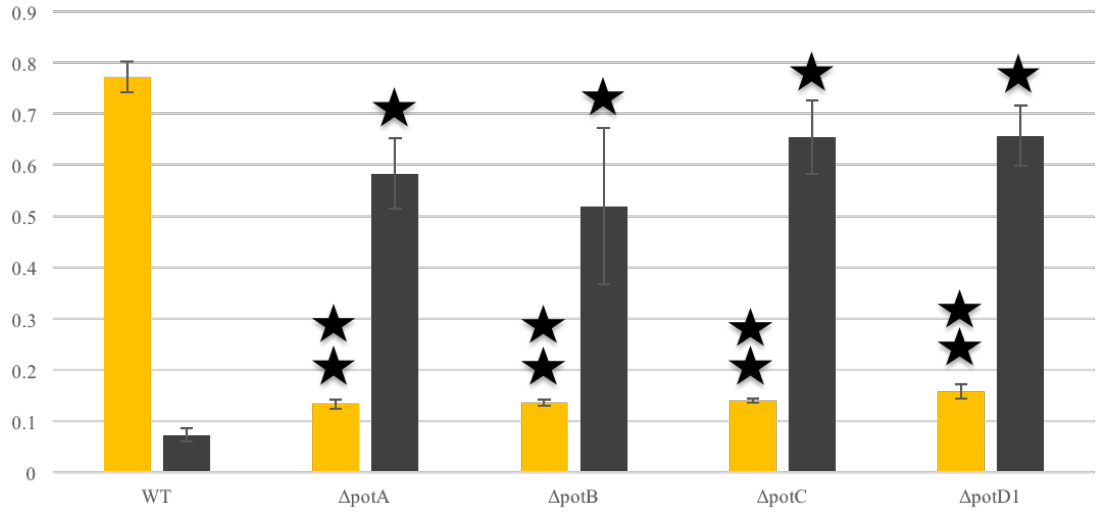

Figure 31. The role of *potABCD1* in biofilm formation. Biofilms were grown at at 27°C without shaking for 24 hours and were quantified by removing planktonic cells, washing with 1X PBS, homogenizing biofilms by vortexing with glass beads, and scoring in a 96-well plate using a spectrophotometer at OD_{655}. One star represents a statistically significant difference between biofilm-associated cell of *pot* mutants and wild type. Two stars represent a statistically significant difference between planktonic cell density of *pot* mutants and wild type. P-values below 0.05 were considered significant. Error bars indicate standard deviation of three biological replicates.

PotA is involved in zebrafish colonization

Because we hypothesize that biofilm formation may be involved in *V. cholerae* association with other organisms, the colonization ability of the biofilm-overproducing Δ*potA* strain was assessed and compared to wildtype. Through serial dilution and plating of intestines, I observed that the Δ*potA* mutant was capable of colonizing the fish intestine at slightly but not significantly higher levels than wildtype *V. cholerae* (Figure 32).

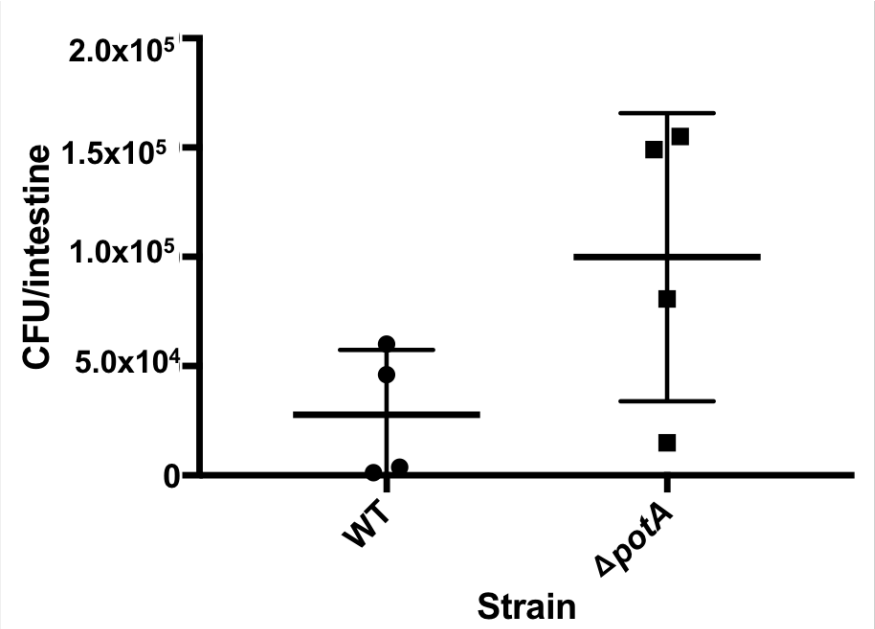

Figure 32. The Δ*potA* mutant colonizes the zebrafish intestine at levels similar to wild type *V. cholerae*. Wild-type and Δ*potA V. cholerae* cells were added in equivalent amounts to fish tanks and incubated overnight. Total mutant and wild type CFUs were calculated by plating serially diluted intestinal homogenates on LB with 100 μM streptomycin and then patching on TCBS agar. One dot represents the intestinal CFU from one fish. Values are normalized to reflect initial inoculation. Student's t-test was performed to determine statistical significance. Error bars reflect the standard deviation of four biological replicates.

Next, I performed the same experiment using a low biofilm forming strain, Δ*nspS* in order to determine if biofilm formation has a role in the ability of *V. cholerae* to colonize the zebrafish intestine. As stated previously, NspS acts to inhibit the phosphodiesterase activity of MbaA, thus increasing the intracellular pool of c-di-GMP. As such, it is a positive regulator of biofilm formation. Therefore, the Δ*nspS* mutant forms very low biofilm compared to wild-type *V. cholerae,* making it a good candidate to test the importance of biofilm formation in fish colonization. As shown in Figure 33, the Δ*nspS* mutant was incapable of colonizing the zebrafish intestine. This was determined to be statistically significant by performing a *t*-test and obtained a *P*-value less than 0.0001. Thus, although formation of biofilm at levels above wildtype may not afford a colonization advantage to *V. cholerae* in the fish intestine, biofilm formation at least to wildtype levels may be required for colonization.

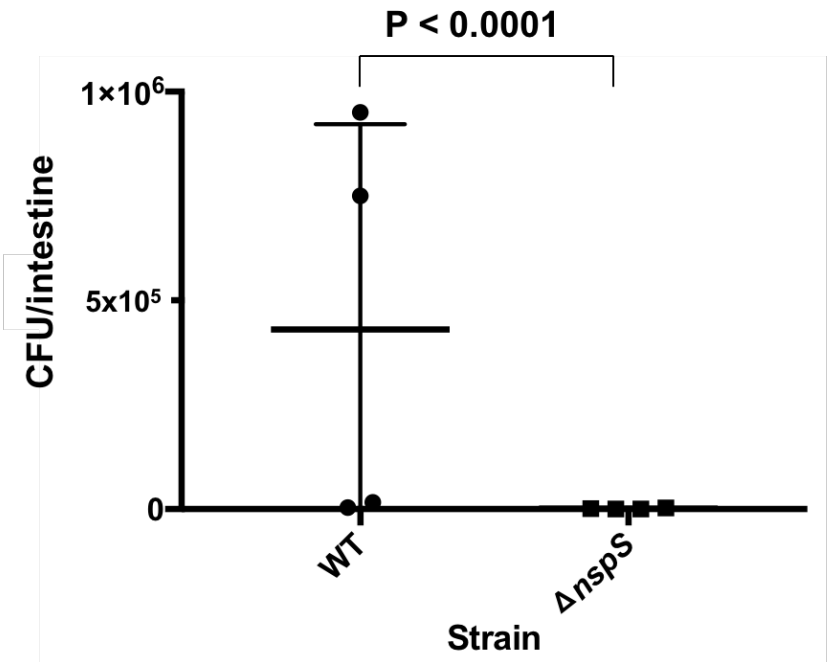

Figure 33. The Δ*nspS* mutant is incapable of colonizing the zebrafish intestine. Wild type and Δ*nspS V. cholerae* cells were added in equivalent amounts to fish tanks and incubated overnight. Total mutant and wild type CFUs were calculated by plating serially diluted intestinal homogenates on LB with 100 μM streptomycin and then patching on TCBS agar. One dot represents the intestinal CFU from one fish. Values are normalized to reflect initial inoculation. Student's t-test was performed to determine statistical significance. Error bars reflect the standard deviation of four biological replicates.

Discussion

In this study, I have characterized the role of the putative ATPase PotA in uptake of the polyamines norspermidine and spermidine in *V. cholerae*. Previous work in the Karatan lab has shown that PotB, PotC and PotD1 are all required to facilitate transport of the triamines norspermidine and spermidine, which then modulate effects on *V. cholerae* biofilm formation through an unknown mechanism (16, 96). The current study confirms the role of PotA in uptake of both polyamines, and supports previous results that spermidine uptake through PotABCD1 inhibits biofilm formation in *V. cholerae.* These results suggest that the entire system functions as a whole in order to facilitate polyamine uptake. Furthermore, this study provides evidence that uptake through PotABCD1 is strongly norspermidine preferential, and provides confirmation that *potABCD2D1* genes are encoded in an operon, and are cotranscribed as a single polycistronic RNA. Altogether, this study provides new information about a novel polyamine transporter in *V. cholerae*.

In order to quantify intracellular norspermidine acquired by the cell only through uptake, the *potA* gene was deleted in the *nspC::kan* mutant background, which is incapable of synthesizing norspermidine *de novo* due to the insertion of a kanamycin resistance cassette in the *nspC* gene. Thus, all intracellular norspermidine in these strains must be imported from the extracellular environment. Through cellular polyamine extraction, benzyolation and HPLC analysis, I observed that deletion of *potA* in the *nspC::kan* background prevented accumulation of intracellular norspermidine when cultures were supplied with 100 μM exogenous norspermidine. This deficiency in norspermidine accumulation could be rescued by complementing the mutant strains with the *potA* gene on a plasmid. Likewise, a deficiency in spermidine import was observed in Δ*potA* single mutant strains, although a small peak was still

present at the retention time seen for spermidine. This could indicate two things; either another low affinity transporter is taking up small amounts of spermidine, or another molecule extracted from the cell has the same retention time as spermidine, and it is removed from the column and read by the HPLC detector at the same time as spermidine. This import-deficient phenotype could be rescued through complementation with the *potA* gene on a plasmid. Recovery of the norspermidine/spermidine peaks in the complemented strains supports the involvement of the PotA protein in uptake of both polyamines.

I also observed an interesting phenomenon in the uptake of spermidine by the Δ*potD1* mutant. Spermidine uptake was greatly diminished, but still present, in the Δ*potA,* Δ*potB,* Δ*potC* strains when supplied with 100 μM spermidine. Previous results in our lab showed that the Δ*potD1* mutant was still capable of taking up spermidine when it was supplied exogenously at 1 mM (20). Consistent with these results, sepermidine uptake in the Δ*potD1* remained uninhibited when cells were supplied with 100 μM of spermidine. Thus, the Δ*potD1* mutant was capable of importing high levels of spermidine in the presence of relatively high, but still physiologically relevant, levels of spermidine, as spermidine can be found in the human intestinal lumen at concentrations of hundreds of micromolar. This implicated the presence of a potential low affinity spermidine transporter, which appears to be capable of binding spermidine when present at high extracellular concentrations and facilitating uptake through the intact PotABC transmembrane and cytoplasmic components. We identified *VCA1113,* which we refer to as *potD3,* as a likely low affinity transporter due to the 43% identity between *potD1* and *potD3* (20). Work is ongoing to generate an in-frame deletion in *potD3* in order to determine if this gene may also have a role in uptake of spermidine through the Pot system under experimental conditions.

Diaminopropane levels also increased consistently in wild-type strains supplied with 100 μM spermidine, Δ*potA* supplemented with 100 μM spermidine, and *nspC::kan* Δ*potA* mutants supplemented with 100 μM norspermidine. The level of diaminopropane was diminished in complemented strains and in wild-type or *nspC::kan* strains supplied with norspermidine. Because diaminopropane is a precursor to carboxynorspermidine, which is itself a precursor to norspermidine, accumulation of diaminopropane in the double mutant strains could be explained by a bottleneck in the norspermidine biosynthesis pathway, resulting in unusually high levels of norspermidine precursors. However, the Δ*potA* single mutant has an intact *nspC* gene, and thus diaminopropane is used for generation of norspermidine, which is verified by a peak at around 24 minutes, the retention time of norspermidine, on the chromatogram of cell extract from the Δ*potA* strain. Therefore, the increase in diaminopropane in this strain is not explained by a biosynthetic bottleneck. It is possible that increased diaminopropane is a result of increased norspermidine synthesis in order to compensate for loss of spermidine. Recently, Kim *et al.* showed that the essential requirement for spermidine in *Agrobacterium tumefaciens* could be replaced by any polyamine that contains a diaminopropane moiety. As such, both diaminopropane and norspermidine were capable of compensating for spermidine. It is unknown if the NspC protein is capable of generating sufficient norspermidine to compensate for a loss of spermidine import through PotABCD. Therefore, it is possible that additional diaminopropane is made in the absence or decrease of spermidine uptake in order to fulfill the usual role of spermidine within the cell.

Because PotABCD1 is capable of importing both norspermidine and spermidine, a substrate preference was investigated. Norspermidine appeared to be the strongly preferred polyamine for import. Even in a 10:1 excess of spermidine, more intracellular norspermidine

than spermidine was detected. Thus, uptake of polyamines through the PotABCD1 system appears to be norspermidine-preferential under the conditions of this experiment.

Because prokaryotic genes with related functions are often under the control of a single promoter, I was also interested in investigating whether the *potABCD2D1* genes are encoded in an operon and are cotranscribed in order to gain more insight into the organization and regulation of this system. RNA was extracted from wild-type *V. cholerae* and reverse-transcribed into cDNA. This cDNA was amplified with primers specific to the intergenic regions, or junctions, between each gene. I observed that the each pair of primers to each gene junction generated a product, indicating that the intergenic regions between each gene in the putative *potABCD2D1* operon are transcribed. This suggests that these five *pot* genes are under the control of a single promoter, and are cotranscribed in one polycistronic RNA.

ABC-transport systems are highly conserved, and have been found to have widespread impact on physiology in prokaryotes. Previous work in our lab has shown that PotB, PotC and PotD1 components effect biofilm formation in *V. cholerae*. In this work, I have shown that PotA is also involved in regulation of *V. cholerae* biofilm formation. Mutations in *potA, potB, potC* or *potD1* result in significantly increased biofilm phenotype compared to wildtype. Because biofilm assays for this study were performed in tryptone media, which contains 3-4μM of spermidine, and because we see a similar increase in biofilm phenotype in each *pot* single mutant, we hypothesize that the disruption of any *pot* gene prevents or diminishes uptake of spermidine into the cell through the PotABCD1 system. This decrease in intracellular spermidine levels is responsible for modulation of biofilm formation, rather than one of the components of the system having a more direct role in biofilm regulation (16). Spermidine has been shown to act as a negative regulator of biofilm formation through the NspS-MbaA sensory

system, through modulation of the second messenger c-di-GMP. Conversely, norspermidine enhances NspS repression of MbaA, which blocks phosphodiesterase activity and leads to an accumulation of c-di-GMP within the cell, leading to increased biofilm formation (16, 51, 68). Thus, spermidine may repress biofilm formation both as an extracellular signal through NspS-MbaA and when accumulated within the cell through the Pot system, indicating that the triamines spermidine and norspermidine may have a profound effect on *V. cholerae* physiology, specifically biofilm formation, through multiple mechanisms.

Finally, because biofilms have been indicated as important in *V. cholerae* environmental survival, and fish have been suggested to serve as an environmental reservoir for *V. cholerae,* I wanted to investigate if polyamine-dependent biofilm formation may be involved in association with other organisms using the zebrafish as a model. Previous work has demonstrated that both adult and larval zebrafish can be naturally colonized by *V. cholerae* following addition of the bacteria to tank water, and are capable of transmitting *V. cholerae* to naive fish. Furthermore, the essential factors required for colonization and infection in humans had no apparent role in the fish colonization (92). I tested the ability of wild-type and the Δ*potA* mutant strains of *V. cholerae* to colonize, and found that Δ*potA* mutants colonized to slightly but not significantly higher levels than wildtype. Conversely, low-biofilm forming Δ*nspS* mutants were extremely deficient in colonization. This may indicate that although high biofilm formation may not necessarily impart a colonization advantage in the fish intestine, biofilm formation may be required to some level in order to colonize. The zebrafish genome encodes a putative spermidine synthase gene, suggesting that cells within the fish may produce spermidine. However, the Δ*potA* mutant was uninhibited in colonization, indicating that spermidine uptake through PotABCD1 may not be essential to survival within the zebrafish. Further investigation of

additional mutants is necessary in order to determine the role of polyamine acquisition and biofilm in fish colonization.

In this study, we have provided further evidence that PotABCD1 is a novel ABC-type transporter, capable of importing both norspermidine and spermidine. Furthermore, we have shown that this system influences *V. cholerae* physiology, modulating biofilm formation through an unknown mechanism. Biofilms formed by prokaryotic bacteria have been shown to protect the cells within from various environmental stressors, from harsh pH and UV irradiation to antimicrobials and even immune system response (22, 27, 65). Bacterial cells within a biofilm are encased within a self-produced matrix and are sessile, making them physiologically distinct from free-swimming cells of the same organism (116). Biofilms have also been shown to provide a colonization advantage in the mouse model, and may provide protection from harsh stomach and bile acid conditions encountered prior to reaching the small intestine (110). Thus, this system may be essential to *V. cholerae* physiology both in the environment and within the human host.

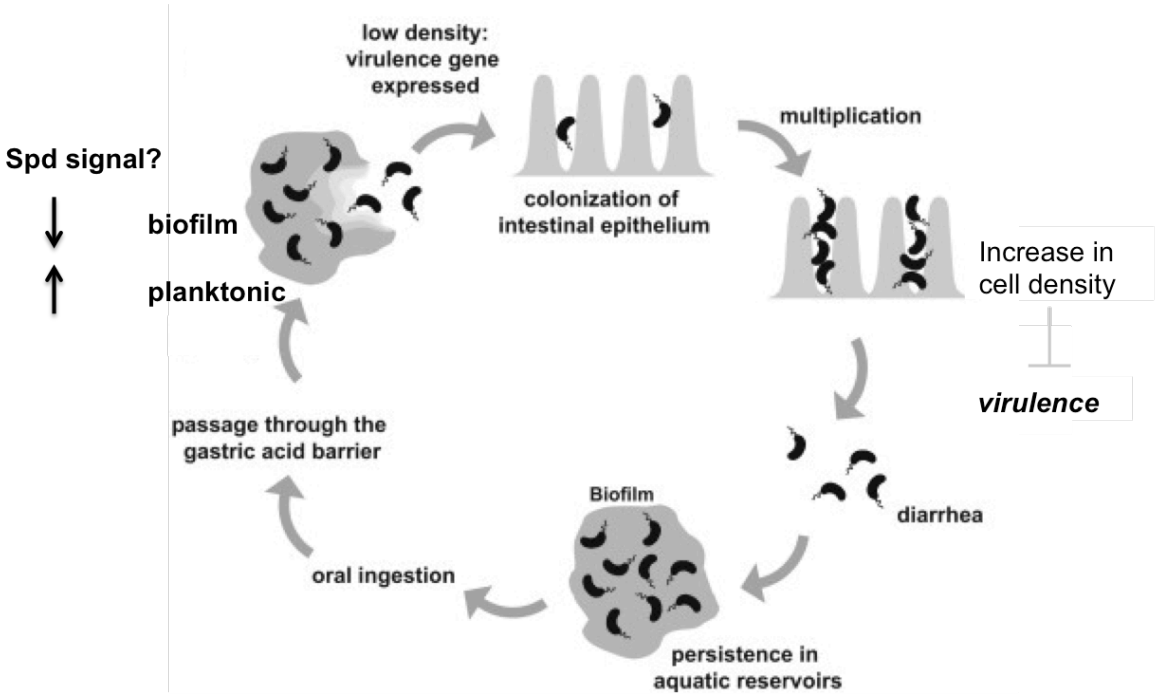

Figure 34. Current model of *V. cholerae* transition between the aquatic environment and human host. *V. cholerae* cells in the environment are thought to persist in biofilms, which also provides protection when ingested. Once bacteria reach the small intestine, an unknown signal causes dispersal from the biofilm, allowing bacteria to begin colonizing the intestinal tissue and expressing virulence genes. Once bacteria leave the body and are returned to the environment, they are thought to reenter the biofilm structure. Modified from Zhu and Mekalanos, 2003.

The current model of *V. cholerae* infection is shown in Figure 34. This model suggests that bacterial cells are typically ingested from environmental sources such as contaminated food or water within a biofilm, and that this structure provides protection from the harsh pH of stomach and bile acids. Therefore, it is thought that *V. cholerae* cells remain in the biofilm until they reach the small intestine, at which point one or more yet unknown signals are encountered, causing bacteria to revert to a planktonic state. The observation that the biofilm-deficient Δ*nspS* mutant was incapable of colonizing the zebrafish provides additional support of the requirement for biofilm in *V. cholerae* association with other organisms. The zebrafish genome also encodes a spermidine synthase gene, indicating the possible presence of spermidine in the fish intestine, although intestinal levels of polyamines in zebrafish are not known. Once out of the biofilm, *V. cholerae* cells begin colonizing the intestinal epithelial cells and producing cholera toxin.

Therefore, consistent with this model, spermidine may serve as an inhibitory signal to biofilm formation and promote a planktonic lifestyle through PotABCD1 and other mechanisms, and contribute to the physiological changes necessary for *V. cholerae* to begin colonizing the intestine and causing the characteristic symptoms of cholera.

References

1. **Absalon, C., K. Van Dellen, and P. I. Watnick.** 2011. A communal bacterial adhesin anchors biofilm and bystander cells to surfaces. PLoS Pathogens **7:**e1002210-e1002210.

2. **Angelichio, M. J., J. Spector, M. K. Waldor, and A. Camilli.** 1999. *Vibrio cholerae* intestinal population dynamics in the suckling mouse model of infection. Infection and Immunity **67:**3733-3739.

3. **Antognoni, F., S. Del Duca, A. Kuraishi, E. Kawabe, T. Fukuchi-Shimogori, K. Kashiwagi, and K. Igarashi.** 1999. Transcriptional inhibition of the operon for the spermidine uptake system by the substrate-binding protein PotD. J Biol Chem **274:**1942-1948.

4. **Bardocz, S., and A. White.** 1999. Polyamines in health and nutrition. Springer Science & Business Media.

5. **Baselski, V., R. Briggs, and C. Parker.** 1977. Intestinal fluid accumulation induced by oral challenge with *Vibrio cholerae* or cholera toxin in infant mice. Infection and Immunity **15:**704-712.

6. **Benyajati, C.** 1966. Experimental cholera in humans. BMJ **1:**140-142.

7. **Blow, N. S., R. N. Salomon, K. Garrity, I. Reveillaud, A. Kopin, F. R. Jackson, and P. I. Watnick.** 2005. *Vibrio cholerae* infection of *Drosophila melanogaster* mimics the human disease cholera. PLoS Pathogens **1:**e8.

8. **Bobrov, A. G., O. Kirillina, and R. D. Perry.** 2005. The phosphodiesterase activity of the HmsP EAL domain is required for negative regulation of biofilm formation in *Yersinia pestis*. FEMS Microbiol Lett **247:**123-130.

9. **Bomchil, N., P. Watnick, and R. Kolter.** 2003. Identification and characterization of a *Vibrio cholerae* gene, mbaA, involved in maintenance of biofilm architecture. J Bacteriol **185:**1384-1390.

10. **Butler, S. M., E. J. Nelson, N. Chowdhury, S. M. Faruque, S. B. Calderwood, and A. Camilli.** 2006. Cholera stool bacteria repress chemotaxis to increase infectivity. Mol Microbiol **60:**417-426.

11. **Casper-Lindley, C., and F. H. Yildiz.** 2004. VpsT is a transcriptional regulator required for expression of vps biosynthesis genes and the development of rugose colonial morphology in *Vibrio cholerae* O1 El Tor. J Bacteriol **186:**1574-1578.

12. **Cassel, D., and Z. Selinger.** 1977. Mechanism of adenylate cyclase activation by cholera toxin: inhibition of GTP hydrolysis at the regulatory site. Proceedings of the National Academy of Sciences **74:**3307-3311.

13. **Cheng, S. H., D. P. Rich, J. Marshall, R. J. Gregory, M. J. Welsh, and A. E. Smith.** 1991. Phosphorylation of the R-Domain by cAMP-dependent protein kinase regulates the CFTR chloride channel. Cell **66:**1027-1036

.

14. **Chiang, S. L., R. K. Taylor, M. Koomey, and J. J. Mekalanos.** 1995. Single amino-acid substitutions in the N-terminus of *Vibrio cholerae* TcpA affect colonization, autoagglutination, and serum resistance. Mol Microbiol **17:**1133-1142.

15. **Choi, A. H., L. Slamti, F. Y. Avci, G. B. Pier, and T. Maira-Litrán.** 2009. The pgaABCD locus of *Acinetobacter baumannii* encodes the production of poly-β-1-6-N-acetylglucosamine, which is critical for biofilm formation. J Bacteriol **191:**5953-5963.

16. **Cockerell, S. R., A. C. Rutkovsky, J. P. Zayner, R. E. Cooper, L. R. Porter, S. S. Pendergraft, Z. M. Parker, M. W. McGinnis, and E. Karatan.** 2014. *Vibrio cholerae* NspS, a homologue of ABC-type periplasmic solute binding proteins, facilitates transduction of polyamine signals independent of their transport. Microbiol-Sgm **160:**832-843.

17. **Cohen, S. S.** 1998. Guide to the polyamines. Oxford University Press.

18. **Colwell, R., and A. Huq.** 2001. Marine ecosystems and cholera. Hydrobiologia **460:**141-145.

19. **Colwell, R. R., and A. Huq.** 1994. Environmental reservoir of *Vibrio cholerae*, the causative agent of cholera. Ann Ny Acad Sci **740:**44-54.

20. **Cooper, R. E.** 2010. NspS, a PotD1 homolog, acts as a spermidine signal sensor, not a transporter, in *Vibrio cholerae*. Appalachian State University .

21. **Costerton, J., Z. Lewandowski, D. DeBeer, D. Caldwell, D. Korber, and G. James.** 1994. Biofilms, the customized microniche. J Bacteriol **176:**2137.

22. **Costerton, J. W., Z. Lewandowski, D. E. Caldwell, D. R. Korber, and H. M. Lappin-Scott.** 1995. Microbial biofilms. Annual Reviews in Microbiology **49:**711-745.

23. **Darby, C., J. W. Hsu, N. Ghori, and S. Falkow.** 2002. *Caenorhabditis elegans*: plague bacteria biofilm blocks food intake. Nature **417:**243-244.

24. **De, S. N., and D. N. Chatterje.** 1953. An experimental study of the mechanism of action of *Vibrio cholerae* on the intestinal mucous membrane. J Pathol Bacteriol **66:**559-562.

25. **Dutta, N., and M. Habbu.** 1955. Experimental cholera in infant rabbits: a method for chemotherapeutic investigation. British Journal of Pharmacology and Chemotherapy **10:**153.

26. **Dziejman, M., D. Serruto, V. C. Tam, D. Sturtevant, P. Diraphat, S. M. Faruque, M. H. Rahman, J. F. Heidelberg, J. Decker, and L. Li.** 2005. Genomic characterization of non-O1, non-O139 *Vibrio cholerae* reveals genes for a type III secretion system. Proceedings of the National Academy of Sciences of the United States of America **102:**3465-3470.

27. **Elasri, M. O., and R. V. Miller.** 1999. Study of the response of a biofilm bacterial community to UV radiation. Appl Environ Microb **65:**2025-2031.

28. **Freter, R., and P. O'Brien.** 1981. Role of chemotaxis in the association of motile bacteria with intestinal mucosa: fitness and virulence of nonchemotactic *Vibrio cholerae* mutants in infant mice. Infection and Immunity **34:**222-233.

29. **Fukuchi, J. I., K. Kashiwagi, M. Yamagishi, A. Ishihama, and K. Igarashi.** 1995. Decrease in cell viability due to the accumulation of spermidine in spermidine acetyltransferase-deficient mutant of *Escherichia coli*. J Biol Chem **270:**18831-18835.

30. **Furuchi, T., K. Kashiwagi, H. Kobayashi, and K. Igarashi.** 1991. Characteristics of the gene for a spermidine and putrescine transport system that maps at 15-min on the *Escherichia coli* chromosome. J Biol Chem **266:**20928-20933.

31. **Galperin, M. Y., A. N. Nikolskaya, and E. V. Koonin.** 2001. Novel domains of the prokaryotic two-component signal transduction systems. FEMS Microbiol Lett **203:**11-21.

32. **Gardel, C. L., and J. J. Mekalanos.** 1996. Alterations in *Vibrio cholerae* motility phenotypes correlate with changes in virulence factor expression. Infection and Immunity **64:**2246-2255.

33. **Gill, D. M., and R. Meren.** 1978. ADP-ribosylation of membrane proteins catalyzed by cholera toxin - basis of activation of adenylate cyclase. Proceedings of the National Academy of Sciences of the United States of America **75:**3050-3054.

34. **Goytia, M., V. L. Dhulipala, and W. M. Shafer.** 2013. Spermine impairs biofilm formation by *Neisseria gonorrhoeae*. FEMS Microbiol Lett **343:**64-69.

35. **Greiner, L., J. Edwards, J. Shao, C. Rabinak, D. Entz, and M. Apicella.** 2005. Biofilm formation by *Neisseria gonorrhoeae*. Infection and Immunity **73:**1964-1970.

36. **Hanahan, D.** 1983. Studies on transformation of *Escherichia coli* with plasmids. J Mol Biol **166:**557-580.

37. **Häse, C. C.** 2001. Analysis of the role of flagellar activity in virulence gene expression in *Vibrio cholerae*. Microbiology **147:**831-837.

38. **Haugo, A. J., and P. I. Watnick.** 2002. *Vibrio cholerae* CytR is a repressor of biofilm development. Mol Microbiol **45:**471-483.

39. **Herrington, D. A., R. H. Hall, G. Losonsky, J. J. Mekalanos, R. K. Taylor, and M. M. Levine.** 1988. Toxin, toxin-coregulated pili, and the ToxR regulon are essential for *Vibrio cholerae* pathogenesis in humans. J Exp Med **168:**1487-1492.

40. **Higashi, K., Y. Sakamaki, E. Herai, R. Demizu, T. Uemura, S. D. Saroj, R. Zenda, Y. Terui, K. Nishimura, T. Toida, K. Kashiwagi, and K. Igarashi.** 2010. Identification and functions of amino acid residues in PotB and PotC involved in spermidine uptake activity. J Biol Chem **285:**39061-39069.

41. **Horton, R. M., Z. Cai, S. N. Ho, and L. R. Pease.** 1990. Gene splicing by overlap extension: tailor-made genes using the polymerase chain reaction. Biotechniques **8:**528-535.

42. **Huq, A., C. A. Whitehouse, C. J. Grim, M. Alam, and R. R. Colwell.** 2008. Biofilms in water, its role and impact in human disease transmission. Current Opinion in Biotechnology **19:**244-247.

43. **Igarashi, K., and K. Kashiwagi.** 2010. Characteristics of cellular polyamine transport in prokaryotes and eukaryotes. Plant Physiol Bioch **48:**506-512.

44. **Igarashi, K., and K. Kashiwagi.** 2010. Modulation of cellular function by polyamines. The International Journal of Biochemistry & Cell Biology **42:**39-51.

45. **Igarashi, K., and K. Kashiwagi.** 2006. Polyamine modulon in *Escherichia coli*: Genes involved in the stimulation of cell growth by polyamines. J Biochem **139:**11-16.

46. **Igarashi, K., K. Kashiwagi, H. Hamasaki, A. Miura, T. Kakegawa, S. Hirose, and S. Matsuzaki.** 1986. Formation of a compensatory polyamine by *Escherichia coli* polyamine-requiring mutants during growth in the absence of polyamines. J Bacteriol **166:**128-134.

47. **Ito, K., and K. Igarashi.** 1986. The increase by spermidine of fidelity of protamine synthesis in a wheat-germ cell-free system. Eur J Biochem **156:**505-510.

48. **Itoh, Y., J. D. Rice, C. Goller, A. Pannuri, J. Taylor, J. Meisner, T. J. Beveridge, J. F. Preston, and T. Romeo.** 2008. Roles of *pgaABCD* genes in synthesis, modification, and export of the *Escherichia coli* biofilm adhesin poly-β-1, 6-N-acetyl-D-glucosamine. J Bacteriol **190:**3670-3680.

49. **Jarrett, C. O., E. Deak, K. E. Isherwood, P. C. Oyston, E. R. Fischer, A. R. Whitney, S. D. Kobayashi, F. R. DeLeo, and B. J. Hinnebusch.** 2004. Transmission of *Yersinia pestis* from an infectious biofilm in the flea vector. J Infect Dis **190:**782-792.

50. **Jones, H. A., J. W. Lillard Jr, and R. D. Perry.** 1999. HmsT, a protein essential for expression of the haemin storage (Hms+) phenotype of *Yersinia pestis*. Microbiology **145:**2117-2128.

51. **Karatan, E., T. R. Duncan, and P. I. Watnick.** 2005. NspS, a predicted polyamine sensor, mediates activation of *Vibrio cholerae* biofilm formation by norspermidine. J Bacteriol **187:**7434-7443.

52. **Kashiwagi, K., H. Endo, H. Kobayashi, K. Takio, and K. Igarashi.** 1995. Spermidine-preferential uptake system in *Escherichia coli* - ATP hydrolysis by PotA protein and its association with membranes. J Biol Chem **270:**25377-25382.

53. **Kashiwagi, K., A. Innami, R. Zenda, H. Tomitori, and K. Igarashi.** 2002. The ATPase activity and the functional domain of PotA, a component of the spermidine-preferential uptake system in *Escherichia coli.* J Biol Chem **277:**24212-24219.

54. **Kashiwagi, K., S. Miyamoto, E. Nukui, H. Kobayashi, and K. Igarashi.** 1993. Functions of PotA and PotD proteins in spermidine-preferential uptake system in *Escherichia coli*. J Biol Chem **268:**19358-19363.

55. **Kashiwagi, K., R. Pistocchi, S. Shibuya, S. Sugiyama, K. Morikawa, and K. Igarashi.** 1996. Spermidine-preferential uptake system in *Escherichia coli* - Identification of amino acids involved in polyamine binding in PotD protein. J Biol Chem **271:**12205-12208.

56. **Kirillina, O., J. D. Fetherston, A. G. Bobrov, J. Abney, and R. D. Perry.** 2004. HmsP, a putative phosphodiesterase, and HmsT, a putative diguanylate cyclase, control Hms-dependent biofilm formation in *Yersinia pestis*. Mol Microbiol **54:**75-88.

57. **Kirn, T. J., M. J. Lafferty, C. M. P. Sandoe, and R. K. Taylor.** 2000. Delineation of pilin domains required for bacterial association into microcolonies and intestinal colonization by *Vibrio cholerae*. Mol Microbiol **35:**896-910.

58. **Klose, K. E.** 2000. The suckling mouse model of cholera. Trends in Microbiology **8:**189-191.

59. **Lee, J., V. Sperandio, D. E. Frantz, J. Longgood, A. Camilli, M. A. Phillips, and A. J. Michael.** 2009. An alternative polyamine biosynthetic pathway is widespread in bacteria and essential for biofilm formation in *Vibrio cholerae*. J Biol Chem **284:**9899-9907.

60. **Lee, S. H., S. M. Butler, and A. Camilli.** 2001. Selection for in vivo regulators of bacterial virulence. Proceedings of the National Academy of Sciences of the United States of America **98:**6889-6894.

61. **Lencer, W. I.** 2004. Retrograde transport of cholera toxin into the ER of host cells. International Journal of Medical Microbiology **293:**491-494.

62. **Lenz, D. H., M. B. Miller, J. Zhu, R. V. Kulkarni, and B. L. Bassler.** 2005. CsrA and three redundant small RNAs regulate quorum sensing in *Vibrio cholerae.* Mol Microbiol **58:**1186-1202.

63. **Lillard, J. W., J. D. Fetherston, L. Pedersen, M. L. Pendrak, and R. D. Perry.** 1997. Sequence and genetic analysis of the hemin storage (hms) system of *Yersinia pestis*. Gene **193:**13-21.

64. **Locher, K. P.** 2009. Structure and mechanism of ATP-binding cassette transporters. Philos T R Soc B **364:**239-245.

65. **Mah, T.-F. C., and G. A. O'Toole.** 2001. Mechanisms of biofilm resistance to antimicrobial agents. Trends in Microbiology **9:**34-39.

66. **Matsumoto, M., and Y. Benno.** 2007. The relationship between microbiota and polyamine concentration in the human intestine: a pilot study. Microbiology and Immunology **51:**25-35.

67. **McEvoy, F., and C. Hartley.** 1975. Polyamines in cystic fibrosis. Pediatric Research **9:**721-724.

68. **McGinnis, M. W., Z. M. Parker, N. E. Walter, A. C. Rutkovsky, C. Cartaya-Marin, and E. Karatan.** 2009. Spermidine regulates *Vibrio cholerae* biofilm formation via transport and signaling pathways. FEMS Microbiol Lett **299:**166-174.

69. **Metcalf, W. W., W. H. Jiang, L. L. Daniels, S. K. Kim, A. Haldimann, and B. L. Wanner.** 1996. Conditionally replicative and conjugative plasmids carrying lacZ alpha for cloning, mutagenesis, and allele replacement in bacteria. Plasmid **35:**1-13.

70. **Metchnikoff, E.** 1894. Recherches sur le cholera et les vibrions. Receptivite des jeunes lapins pour le cholera intestinal. Ann. Inst. Pasteur (Paris) **8:**557.

71. **Miller, V. L., and J. J. Mekalanos.** 1988. A novel suicide vector and its use in construction of insertion mutations - osmoregulation of outer-membrane proteins and virulence determinants in *Vibrio cholerae* requires ToxR. J Bacteriol **170:**2575-2583.

72. **Miller, V. L., and J. J. Mekalanos.** 1984. Synthesis of cholera toxin is positively regulated at the transcriptional level by *toxR*. Proceedings of the National Academy of Sciences **81:**3471-3475.

73. **Milovic, V.** 2001. Polyamines in the gut lumen: bioavailability and biodistribution. Eur J Gastroen Hepat **13:**1021-1025.

74. **Mondragón, V., B. Franco, K. Jonas, K. Suzuki, T. Romeo, Ö. Melefors, and D. Georgellis.** 2006. pH-dependent activation of the BarA-UvrY two-component system in *Escherichia coli*. J Bacteriol **188:**8303-8306.

75. **Murphy, G. M.** 2001. Polyamines in the human gut. Eur J Gastroen Hepat **13:**1011-1014.

76. **Nakao, H., S. Shinoda, and S. Yamamoto.** 1991. Purification and some properties of carboxynorspermidine synthase participating in a novel biosynthetic pathway for norspermidine in *Vibrio alginolyticus*. Microbiology **137:**1737-1742.

77. **Nesse, L. L., K. Berg, and L. K. Vestby.** 2015. Effects of norspermidine and spermidine on biofilm formation by potentially pathogenic *Escherichia coli* and *Salmonella enterica* wild-type strains. Appl Environ Microb **81:**2226-2232.

78. **Ogasawara, H., K. Yamada, A. Kori, K. Yamamoto, and A. Ishihama.** 2010. Regulation of the *Escherichia coli* csgD promoter: interplay between five transcription factors. Microbiology **156:**2470-2483.

79. **Olivier, V., J. Queen, and K. Satchell.** 2009. Successful small intestine colonization of adult mice by *Vibrio cholerae* requires ketamine anesthesia and accessory toxins. PloS one **4:**e7352.

80. **Olivier, V., N. H. Salzman, and K. J. F. Satchell.** 2007. Prolonged colonization of mice by *Vibrio cholerae* El Tor O1 depends on accessory toxins. Infection and Immunity **75:**5043-5051.

81. **Osborne, D. L., and E. R. Seidel.** 1990. Gastrointestinal luminal polyamines: cellular accumulation and enterohepatic circulation. Am J Physiol-Gastr L **258:**G576-G584.

82. **Parker, Z. M., S. S. Pendergraft, J. Sobieraj, M. M. McGinnis, and E. Karatan.** 2012. Elevated levels of the norspermidine synthesis enzyme NspC enhance *Vibrio cholerae* biofilm formation without affecting intracellular norspermidine concentrations. FEMS Microbiol Lett **329:**18-27.

83. **Patel, C. N., B. W. Wortham, J. L. Lines, J. D. Fetherston, R. D. Perry, and M. A. Oliveira.** 2006. Polyamines are essential for the formation of plague biofilm. J Bacteriol **188:**2355-2363.

84. **Pernestig, A.-K., Ö. Melefors, and D. Georgellis.** 2001. Identification of UvrY as the cognate response regulator for the BarA sensor kinase in *Escherichia coli.* J Biol Chem **276:**225-231.

85. **Perry, R. D., A. G. Bobrov, O. Kirillina, H. A. Jones, L. Pedersen, J. Abney, and J. D. Fetherston.** 2004. Temperature regulation of the hemin storage (Hms+) phenotype of *Yersinia pestis* is posttranscriptional. J Bacteriol **186:**1638-1647.

86. **Purdy, A. E., and P. I. Watnick.** 2011. Spatially selective colonization of the arthropod intestine through activation of *Vibrio cholerae* biofilm formation. Proceedings of the National Academy of Sciences of the United States of America **108:**19737-19742.

87. **Rashid, M. H., C. Rajanna, A. Ali, and D. K. Karaolis.** 2003. Identification of genes involved in the switch between the smooth and rugose phenotypes of *Vibrio cholerae*. FEMS Microbiol Lett **227:**113-119.

88. **Richardson, K.** 1991. Roles of motility and flagellar structure in pathogenicity of *Vibrio cholerae*: analysis of motility mutants in three animal models. Infection and Immunity **59:**2727-2736.

89. **Richardson, S. H.** 1994. Animal models in cholera research. *Vibrio cholerae* and cholera: molecular to global perspectives. ASM Press, Washington, DC**:**203-226.

90. **Ritchie, J. M., H. Rui, R. T. Bronson, and M. K. Waldor.** 2010. Back to the future: studying cholera pathogenesis using infant rabbits. mBio **1:**e00047-00010.

91. **Romeo, T.** 1998. Global regulation by the small RNA-binding protein CsrA and the non-coding RNA molecule CsrB. Mol Microbiol **29:**1321-1330.

92. **Runft, D. L., K. C. Mitchell, B. H. Abuaita, J. P. Allen, S. Bajer, K. Ginsburg, M. N. Neely, and J. H. Withey.** 2014. Zebrafish as a natural host model for *Vibrio cholerae* colonization and transmission. Appl Environ Microb **80:**1710-1717.

93. **Sack, D. A., R. B. Sack, G. B. Nair, and A. K. Siddique.** 2004. Cholera. Lancet **363:**223-233.

94. **Sakamoto, A., Y. Terui, T. Yamamoto, T. Kasahara, M. Nakamura, H. Tomitori, K. Yamamoto, A. Ishihama, A. J. Michael, and K. Igarashi.** 2012. Enhanced biofilm formation and/or cell viability by polyamines through stimulation of response regulators UvrY and CpxR in the two-component signal transducing systems, and ribosome recycling factor. The International Journal of Biochemistry & Cell Biology **44:**1877-1886.

95. **Sanchez, J., and J. Holmgren.** 2008. Cholera toxin structure, gene regulation and pathophysiological and immunological aspects. Cell Mol Life Sci **65:**1347-1360.

96. **Sanders, B. E.** 2015. Characterization of the norspermidine/spermidine ABC-type transporter, PotABCD1, in *Vibrio cholerae*. Appalachian State University.

97. **Schlech, W. F., D. P. Chase, and A. Badley.** 1993. A model of food-borne Listeria monocytogenes infection in the Sprague-Dawley rat using gastric inoculation: development and effect of gastric acidity on infective dose. International Journal of Food Microbiology **18:**15-24.

98. **Schuhmacher, D. A., and K. E. Klose.** 1999. Environmental signals modulate ToxT-dependent virulence factor expression in *Vibrio cholerae*. J Bacteriol **181:**1508-1514.

99. **Senderovich, Y., I. Izhaki, and M. Halpern.** 2010. Fish as reservoirs and vectors of *Vibrio cholerae*. PloS one **5:**e8607.

100. **Senior, A. E., and S. Bhagat.** 1998. P-glycoprotein shows strong catalytic cooperativity between the two nucleotide sites. Biochemistry-Us **37:**831-836.

101. **Shah, P., and E. Swlatlo.** 2008. A multifaceted role for polyamines in bacterial pathogens. Mol Microbiol **68:**4-16.

102. **Shukla, B., D. Singh, and S. Sanyal.** 1995. Attachment of non-culturable toxigenic *Vibrio cholerae* O1 and non-O1 and *Aeromonas* spp. to the aquatic arthropod *Gerris spinolae* and plants in the River Ganga, Varanasi. FEMS Immunology and Medical Microbiology **12:**113-120.

103. **Simm, R., J. D. Fetherston, A. Kader, U. Römling, and R. D. Perry.** 2005. Phenotypic convergence mediated by GGDEF-domain-containing proteins. J Bacteriol **187:**6816-6823.

104. **Spira, W., R. Sack, and J. Froehlich.** 1981. Simple adult rabbit model for *Vibrio cholerae* and enterotoxigenic *Escherichia coli* diarrhea. Infection and Immunity **32:**739-747.

105. **Subramanya, S. B., V. M. Rajendran, P. Srinivasan, N. S. N. Kumar, B. S. Ramakrishna, and H. J. Binder.** 2007. Differential regulation of cholera toxin-inhibited Na-H exchange isoforms by butyrate in rat ileum. Am J Physiol-Gastr L **293:**G857-G863.

106. **Tabor, C. W., and H. Tabor.** 1984. Polyamines. Annu Rev Biochem **53:**749-790.

107. **Tacket, C. O., R. K. Taylor, G. Losonsky, Y. Lim, J. P. Nataro, J. B. Kaper, and M. M. Levine.** 1998. Investigation of the roles of toxin-coregulated pili and mannose-sensitive hemagglutinin pili in the pathogenesis of *Vibrio cholerae* O139 infection. Infection and Immunity **66:**692-695.

108. **Tait, G. H.** 1976. A new pathway for the biosynthesis of spermidine. Biochemical Society Transactions **4:**610-612.

109. **Tamamoto, T., K. Nakashima, N. Nakasone, Y. Honma, N. Higa, and T. Yamashiro.** 1998. Adhesive property of toxin-coregulated pilus of *Vibrio cholerae* O1. Microbiology and Immunology **42:**41-45.

110. **Tamayo, R., B. Patimalla, and A. Camilli.** 2010. Growth in a biofilm induces a hyperinfectious phenotype in *Vibrio cholerae*. Infection and Immunity **78:**3560-3569.

111. **Taylor, R. K., V. L. Miller, D. B. Furlong, and J. J. Mekalanos.** 1987. Use of *phoA* gene fusions to identify a pilus colonization factor coordinately regulated with cholera toxin. Proceedings of the National Academy of Sciences of the United States of America **84:**2833-2837.

112. **Tischler, A. D., and A. Camilli.** 2004. Cyclic diguanylate (c-di-GMP) regulates *Vibrio cholerae* biofilm formation. Mol Microbiol **53:**857-869.

113. **Tyms, A.** 1989. Polyamines and the growth of bacteria and viruses. The Physiology of Polyamines **2:**368.

114. **Vlamakis, H., Y. Chai, P. Beauregard, R. Losick, and R. Kolter.** 2013. Sticking together: building a biofilm the *Bacillus subtilis* way. Nature Reviews Microbiology **11:**157-168.

115. **Waldor, M. K., and J. J. Mekalanos.** 1996. Lysogenic conversion by a filamentous phage encoding cholera toxin. Science **272:**1910-1914.

116. **Watnick, P., and R. Kolter.** 2000. Biofilm, city of microbes. J Bacteriol **182:**2675-2679.

117. **Watnick, P. I., and R. Kolter.** 1999. Steps in the development of a *Vibrio cholerae* El Tor biofilm. Mol Microbiol **34:**586-595.

118. **Weilbacher, T., K. Suzuki, A. K. Dubey, X. Wang, S. Gudapaty, I. Morozov, C. S. Baker, D. Georgellis, P. Babitzke, and T. Romeo.** 2003. A novel sRNA component of the carbon storage regulatory system of *Escherichia coli*. Mol Microbiol **48:**657-670.

119. **Wortham, B. W., M. A. Oliveira, J. D. Fetherston, and R. D. Perry.** 2010. Polyamines are required for the expression of key Hms proteins important for *Yersinia pestis* biofilm formation. Environ Microbiol **12:**2034-2047.

120. **Xu, Q., M. Dziejman, and J. J. Mekalanos.** 2003. Determination of the transcriptome of Vibrio cholerae during intraintestinal growth and midexponential phase in vitro. Proceedings of the National Academy of Sciences **100:**1286-1291.

121. **Yamamoto, K., and A. Ishihama.** 2006. Characterization of copper-inducible promoters regulated by CpxA/CpxR in *Escherichia coli.* Bioscience, biotechnology, and biochemistry **70:**1688-1695.

122. **Yamamoto, K., and A. Ishihama.** 2005. Transcriptional response of *Escherichia coli* to external copper. Mol Microbiol **56:**215-227.

123. **Yamamoto, S., K. Hamanaka, Y. Suemoto, B.-i. Ono, and S. Shinoda.** 1986. Evidence for the presence of a novel biosynthetic pathway for norspermidine in Vibrio. Can J Microbiol **32:**99-103.

124. **Yamamoto, S., S. Shinoda, M. Kawaguchi, K. Wakamatsu, and M. Makita.** 1983. Polyamine distribution in vibrionaceae - norspermidine as a general constituent of Vibrio Species. Can J Microbiol **29:**724-728.

125. **Yildiz, F. H., N. A. Dolganov, and G. K. Schoolnik.** 2001. VpsR, a member of the response regulators of the two-component regulatory systems, is required for expression of *vps* biosynthesis genes and EPS^{ETr}-associated phenotypes in *Vibrio cholerae* O1 El Tor. J Bacteriol **183:**1716-1726.

126. **Yoshida, M., K. Kashiwagi, A. Shigemasa, S. Taniguchi, K. Yamamoto, H. Makinoshima, A. Ishihama, and K. Igarashi.** 2004. A unifying model for the role of polyamines in bacterial cell growth, the polyamine modulon. J Biol Chem **279:**46008-46013.

127. **Yoshida, M., D. Meksuriyen, K. Kashiwagi, G. Kawai, and K. Igarashi.** 1999. Polyamine stimulation of the synthesis of oligopeptide-binding protein (OppA) - Involvement of a structural change of the Shine-Dalgarno sequence and the initiation codon AUG in OppA mRNA. J Biol Chem **274:**22723-22728.

128. **Zhang, R. G., D. L. Scott, M. L. Westbrook, S. Nance, B. D. Spangler, G. G. Shipley, and E. M. Westbrook.** 1995. The 3-dimensional crystal structure of cholera toxin. J Mol Biol **251:**563-573.

Vita

Elizabeth Anne Villa was born in Fairfax, Virginia. After graduating from Briar Woods High School in Ashburn, Virginia, she attended Virginia Polytechnic Institute and State University, earning a Bachelor of Science in Biological Sciences. She began pursuit of a Master of Science in Biology with a concentration in Cell and Molecular Biology at Appalachian State University, as well as working in Dr. Ece Karatan's laboratory in the fall of 2014. Upon completion of her Master of Science, she will pursue a doctoral degree in Microbiology at the University of Georgia.